Supplementary Figure S1. Exatecan cytotoxicity and sensitivity to multidrug resistant genes.

A. Structure of exatecan and DXd. Red oval highlights the structural modification of exatecan on the NH_2 (on F ring) by a 2-hydroxyacetyl group ($CO\text{-}CH_2\text{-}OH$) to become more hydrophilic DXd.

B. Cytotoxicity of exatecan compared to DXd. Cells were incubated with a concentration series of exatecan or DXd for 5 days. Cell viability was measured by CCK8 and IC_{50} for each cell line was calculated from cell viability-concentration plot. Cell lines were grouped for each labeled tumor type. Data represent 3 independent measurements.

C. Detection of DNA-trapped TOP1 by exatecan, DXd and SN-38. DNA staining as loading control for the RADAR assay shown in Fig. 1A-1B.

D. Lipophilic ligand efficiency (LLE) calculation. The average IC_{50} for exatecan/SN-38/DXd was used. LLE = pIC_{50} (avg.) - $LogD_{7.0}$ and $LogD_{7.0}$ values were predicted by using ChemAxon LogD Predictor (https://disco.chemaxon.com/calculators/demo/plugins/logd/).

E. The measurement of efflux of exatecan and DXd/SN-38 in Caco-2 cells. The permeability rates and efflux ratios of digoxin and erythromycin Estrone 3-Sulfate sodium salt were used as positive controls. Inhibitors used were listed in the table. Values represent mean$\pm$S.D.; n = 3 replicates in >=3 assays in each experimental group.

F. Absorbance/emission scan of exatecan and DXd.

G. ABCG2 expression in cell lines by flow cytometry relative to an isotype IgG control. Cell lines are represented by different colors shown on the right.

H. H-J. Representative fluorescence images of intracellular accumulation of exatecan and DXd in HCI-H460 after a 4-hour incubation of cells with drugs. D. In COLO205, exatecan (Top Right) and DXd (Top Left) accumulated similarly and was not affected by ABCG2 inhibitor Resperpine (Bottom). E. In NCI-H460, no accumulation of DXd (Top, Middle; Left is the cells in the same area observed in the brightfield) was not affected by p-gp inhibitor Verapamil and accumulation of exatecan was not affected (Top Right). Double inhibition of ABCG2 and p-gp (Bottome Middle and Left) had similar effect as ABCG2 inhibition alone (see Fig. 1C Bottom Middle). F. NCI-H460 cells were not fluorescent with Reserpine (Top Right) or Verapamil alone (Bottom Right). Brightfield of cells in the same area are shown as controls. Scale bar, 20 µM.

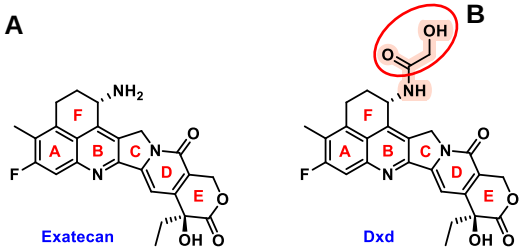

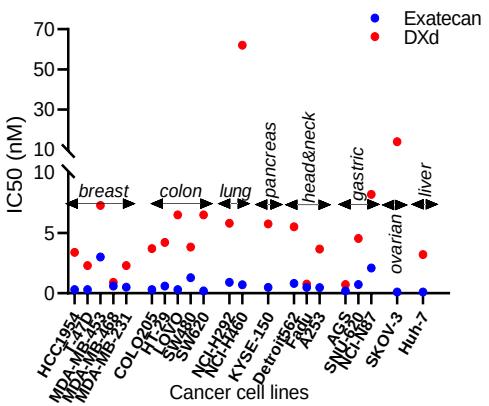

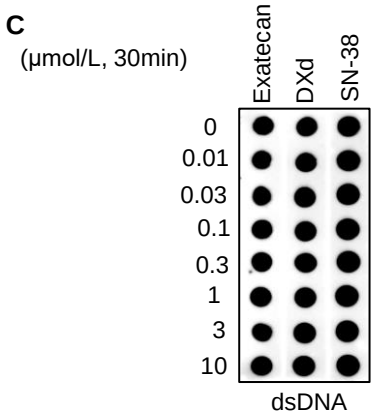

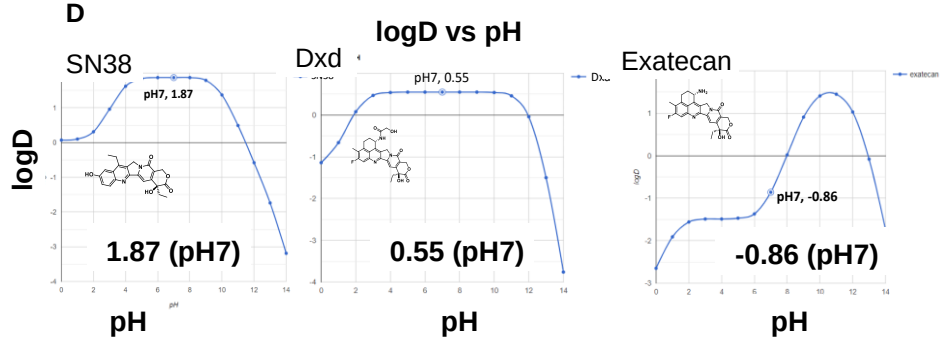

	$IC_{50\,(avg.)}$ nM	$pIC_{50(avg.)}$	$LogD_{7.0}$ [a]	LLE[b]
SN38	*5.2*	8.28	1.87	**6.41**
Dxd	*6.9*	8.16	0.55	**7.61**
Exatecan	*0.6*	9.22	-0.86	**10.08**

E

Compound ID	Inhibitor*	Permeability (10^{-6} cm/s) A to B	Permeability (10^{-6} cm/s) B to A	Efflux Ratio	Compound ID	Inhibitor*	Permeability (10^{-6} cm/s) A to B	Permeability (10^{-6} cm/s) B to A	Efflux Ratio
Estrone 3-Sulfate Sodium Salt#	-	0.408	6.315	15.5	Digoxin$	-	0.267	8.283	31.0
	GF120918	NA	NA	NA		GF120918	2.749	2.579	0.9
	Novobiocin	1.961	2.336	1.2		Verapamil	2.915	2.719	0.9
Exatecan	-	2.14±0.27	11.00±0.80	5.1	Exatecan	-			
	GF120918	7.88±1.22	3.23±0.09	0.4		GF120918			
	Novobiocin	4.22±0.28	6.1±1.53	1.4		Verapamil	5.43±1.17	7.38±0.50	1.4
DXd	-	0.19±0.02	7.23±0.21	37.5	DXd	-			
	GF120918	0.66±0.10	4.18±0.20	6.3		GF120918			
	Novobiocin	0.31±0.03	4.42±0.89	14.5		Verapamil	0.18±0.06	5.57±1.28	30.2
SN-38	-	0.13±0.10	1.61±0.35	12.4	SN-38	-			
	GF120918	0.57±0.06	0.86±0.15	1.5					
	Novobiocin	0.38±0.16	1.07±0.21	2.8		Verapamil	0.16±0.02	1.41±0.12	8.7

 # a positive control as an ABCG2 substrate
$ a positive control as a p-gp substrate
** Inhibitor class: GF120918 for both ABCG-2 and p-gp; Novobiocin for ABCG-2; Verapamil for p-gp*

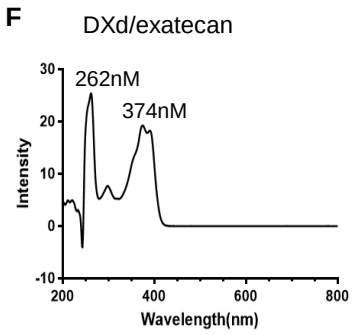

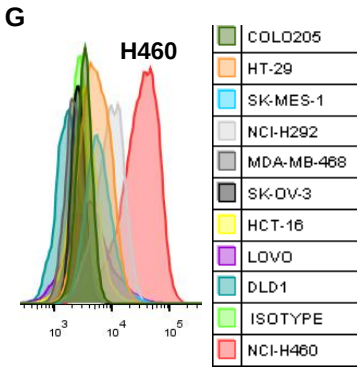

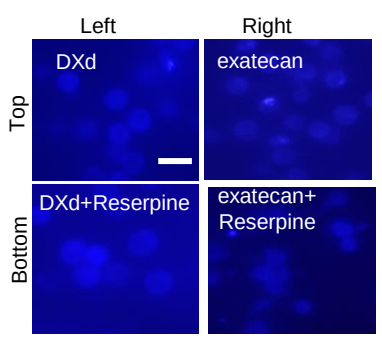

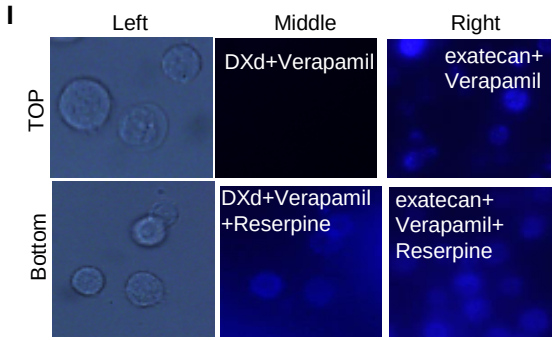

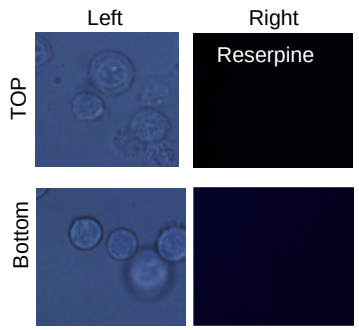

Supplementary Figure S2. Exatecan and DXd/SN-38 sensitivity to multidrug resistant genes.

A-C. P-gp and ABCG2 mRNA expression from Cancer Cell Line Encyclopedia (CCLE) at https://sites.broadinstitute.org/ccle/ and protein expression by flow cytometry. A. ABCG2/p-gp high and low expression cells were defined as top and bottom 20-30% expressors in the database (tabulated on the top of the graph). B. Correlation of mRNA and cell surface protein expression of ABCG2. ABCG2 protein expression was measured by a mouse anti-ABCG2 antibody by flow cytometry. C. Two cell lines with high mRNA and cell surface protein expression of p-gp. No correlation of mRNA and cell surface protein expression of p-gp was found except in a few high pgp mRNA expression cell lines.

D,E. IC_{50} ratio of DXd/exatecan and ABCG2 (D) and p-gp (E) mRNA expression based on data from Fig.S1B and Fig.S1F-S1H. Cell lines with green colors were cell lines with high expression of both ABCG2 and p-gp and were excluding from the plot in Fig. 1F in ABCG2 high and pgp high groups. Cell lines with light yellow colors were excluded in the low expression group for plotting Fig.1F.

F,G. ABCG2 and p-gp inhibitor sensitizes cancer cell lines to DXd/SN-38. H2710 (F) (ABCG2 high) cytotoxicity with exatecan, DXd and SN-38 with/without 2 μM of YHO-13177 was compared. Tariquidar (5 μM) was used as p-gp inhibitor for HCT-15 (G) with high p-gp expression. Data represent 2 independent measurements. Change of IC_{50} is shown in Fig.1G.

A

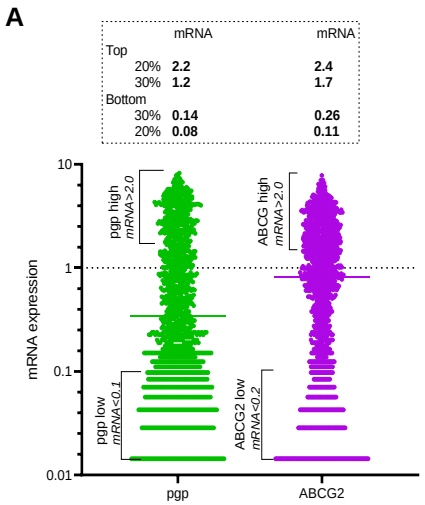

B

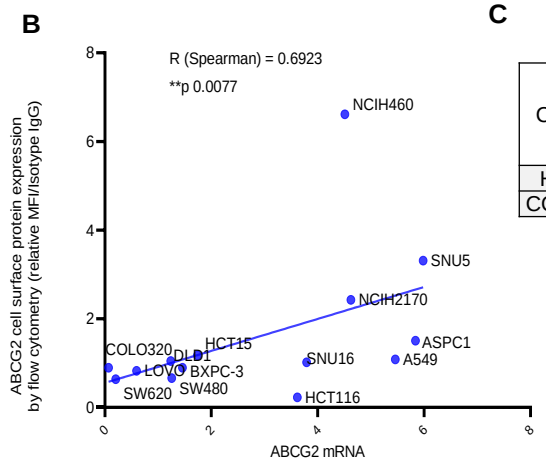

C

Cell line	ABCB1/pgp expression	
	mRNA	Cell surface protein (relative MFI/Isotype IgG)
HCT15	6.8	24
COLO320	7.7	70

D

Cell line	DXd/exatecan	ABCG2
HCC1954	11.3	2.154
MDA-MB-231	4.6	3.716
HT-29	7.1	4.114
LOVO	*21.7*	*3.618*
NCI-H292	6.4	3.430
NCI-H460	*88.6*	*4.512*
KYSE-150	11.7	3.610
SNU-620	6.2	2.508
Huh-7	*32.0*	*2.674*
T-47D	7.7	0.124
MDA-MB-453	2.4	0.000
MDA-MB-468	1.5	0.151
SW480	3.0	0.202
SW620	*32.5*	*0.070*
Detroit562	*6.8*	*0.807*
Fadu	*1.6*	*0.454*
AGS	*3.8*	*0.275*
NCI-N87	*3.9*	*0.227*

E

Cell line	DXd/exatecan	pgp
LOVO	*21.7*	*4.958*
SW620	32.5	2.198
NCI-H460	*88.6*	*2.236*
Huh-7	*32.0*	*4.572*
HCC1954	*11.3*	*0.111*
T-47D	7.7	0.057
MDA-MB-453	2.4	0.014
MDA-MB-468	*1.5*	*1.269*
MDA-MB-231	*4.6*	*0.057*
HT-29	*7.1*	*0.138*
SW480	*3.0*	*0.856*
NCI-H292	*6.4*	*0.070*
KYSE-150	*11.7*	*0.043*
Detroit562	6.8	0.014
Fadu	*1.6*	*1.131*
A253	*7.8*	*0.401*
AGS	*3.8*	*0.239*
SNU-620	6.2	0.084
NCI-N87	*3.9*	*0.111*
SKOV-3	*140.0*	*0.251*

F

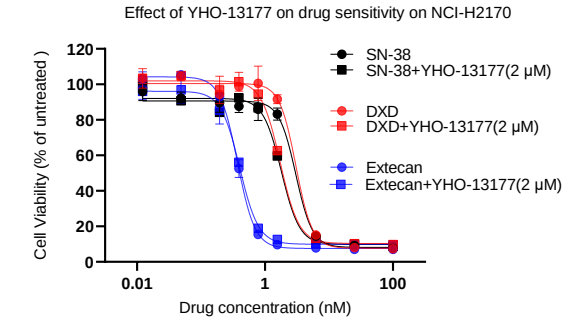

G

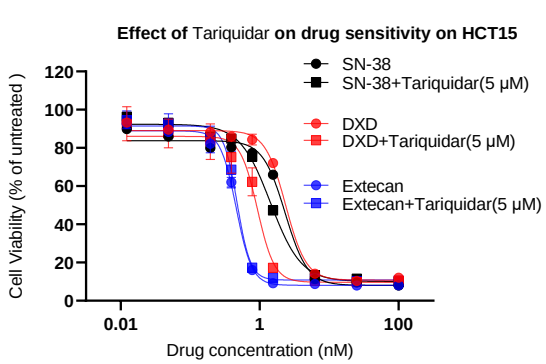

Supplementary Figure S3. Exatecan toxicity in rat.

Rat toxicity study. Six rats were given 3, 10, 30 mg/kg of exatecan mesylate on day 1, 8, 15, 22, and 29 (shown as red arrows in A) and with a 4-week recovery period (3 of 6 animals).

A. Body weight change percentage. Dashed line indicates starting body weight.

B. Count of white blood cells.

C. Count of neutrophils.

D, E. Hematology results were shown for after 5 infusions (six rats) and after 4-week recovery (3 rats). D. Count of red blood cells. E. Count of lymphocytes.

F, G. Serum chemistry. F. Serum alanine aminotransferase level. G. Serum aspartate aminotransferase level.

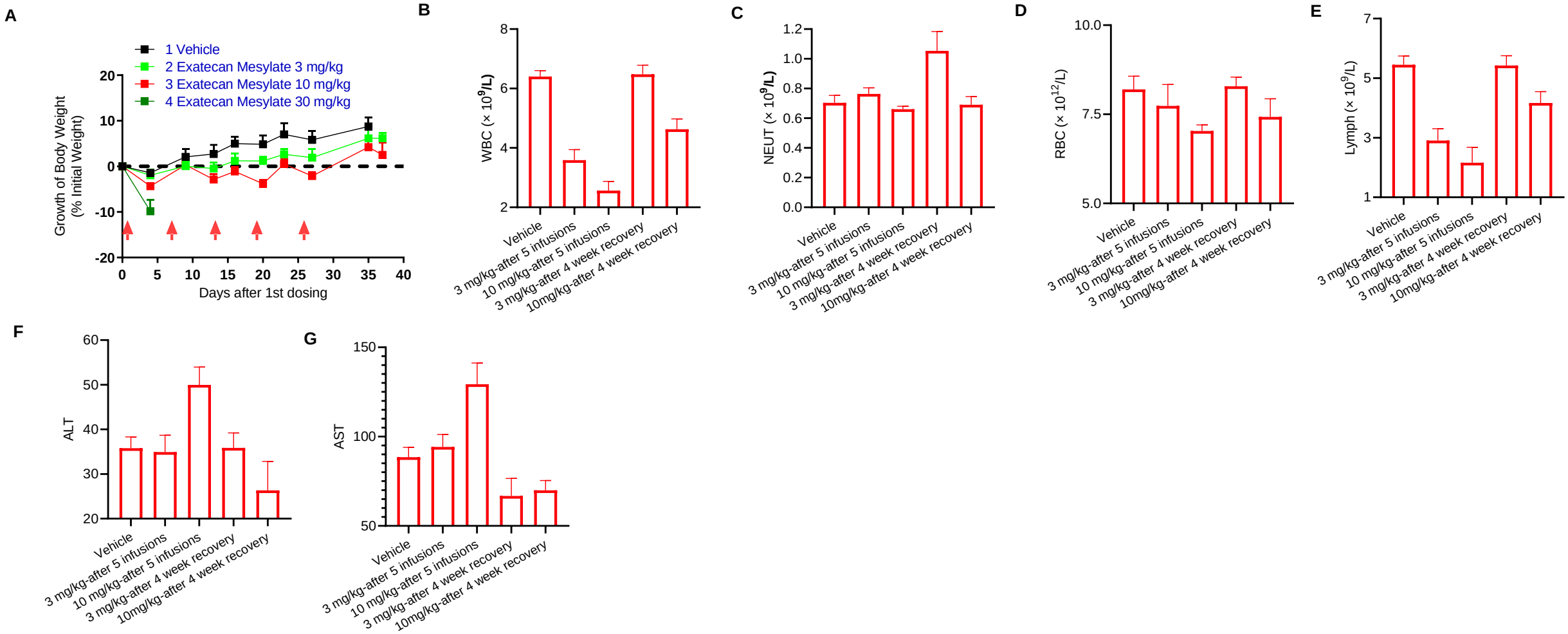

Supplementary Figure S4. The design and optimization of T moiety.

A. The process of T moiety selection and optimization. Commonly used peptide linkers were in S0. Modification site at MC/linker (called M moiety) or PAB (called T moiety) was shown in Structure 1 (S1). PEG was first used to modify MC or PAB to yield M900 (S2) or T900 (S3). Replacing PEG with methylaminomethyl or polysarcosine (pSAR) produced additional T moieties T800 and T1000 (S4). Modification of peptide linker VA with a similarly hydrophilic amine-containing group (butylamine) as methylaminomethyl resulted in VK (M800 in S5). Physicochemical profiles of HER2-targeting ADCs by conjugating Trastuzumab (Tras) with exatecan using each M and T moiety were compared to select T1000 (T800) as optimal structures for antibody-exatecan conjugates.

B. Structure-aggregation relationship of T moiety-exatecan ADCs analyzed by SEC. Antibody is HER2 targeting Trastuzumab (Tras).

C. Hydrophilicity score of T moiety derived from PABC modification. CLogP is calculated as described in Buecheler JW, Winzer M, Tonillo J, Weber C, Gieseler H. Impact of Payload Hydrophobicity on the Stability of Antibody-Drug Conjugates. Mol Pharm.15, 2656-2664 (2018).

A

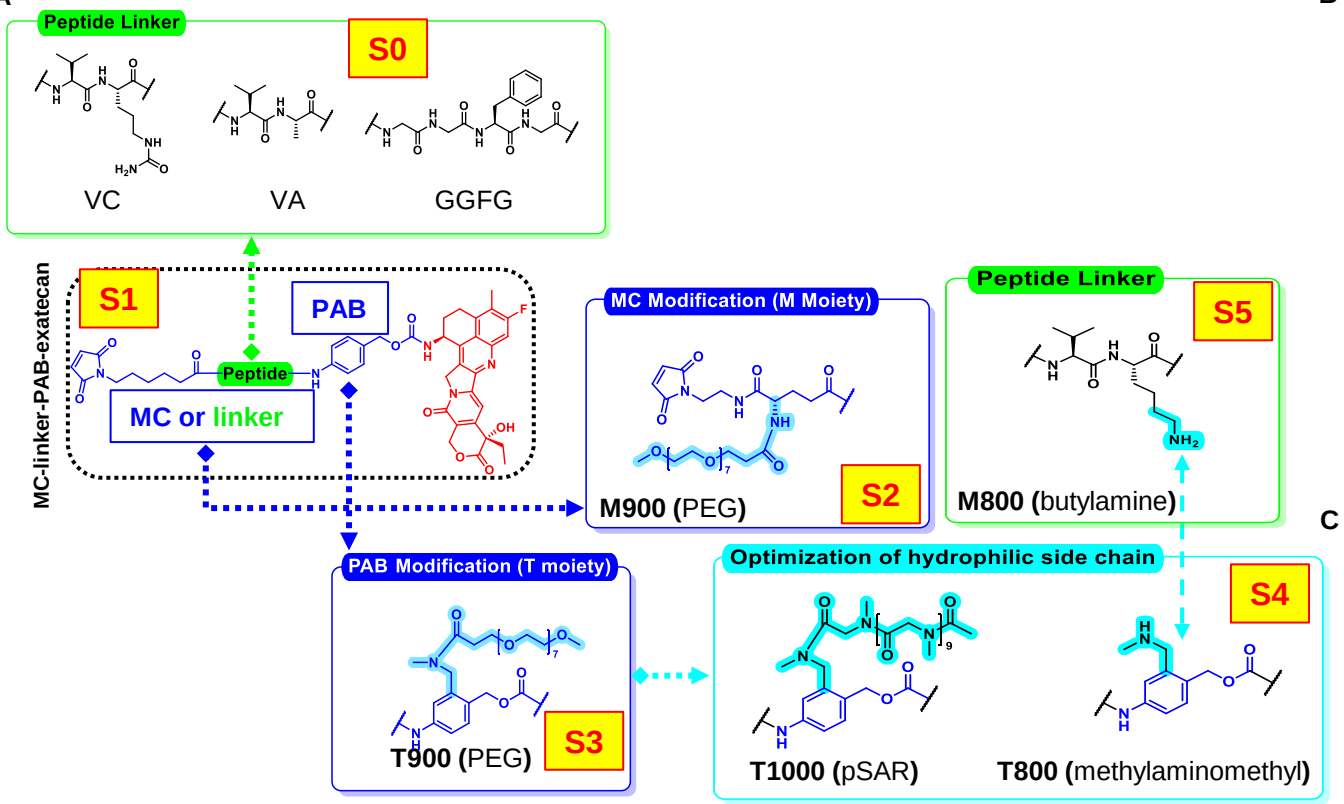

B

	Structural identification	MC-peptide linker-PAB-exatecan structure	ADC characterization	
			DAR	Aggregation rate (%)
Unmodified peptide linker	VC	Mc-VC-PABC-e	4-8	> 50
	VA	Mc-VA-PABC-e		> 50
	GGFG	Mc-GGFG-PABC-e		> 50
M moiety: *MC or peptide linker modification*	M800 (VK)	Mc-VK-PABC-e	8	20
	M900 (PEG)	M'(PEG_8-OMe)-VA-PABC-e		>50
T moiety: *PAB modification*	T800 (methylaminomethyl)	Mc-VA-PABC'-e	8	2.8
	T900 (PEG)	Mc-VA-PABC'(PEG_8-OMe)-e		0.9
	T1000 (pSAR)	Mc-VA-PABC'($pSAR_{10}$)-e		0.64
	T1001 (GGFG/pSAR)	Mc-GGFG-PABC'($pSAR_{10}$)-e		1.8

C

PABC modification	Structure	T Moiety	CLogP
none	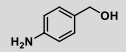		0.478
CH_2-NH-CH_3	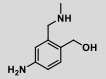	T800	0.016
CH_2-N-(=O-PEG_8-OMe)-CH_3	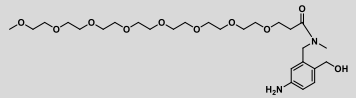	T900	-1.12
x= CH_2-N-(=O-$pSAR_{10}$)-CH_3	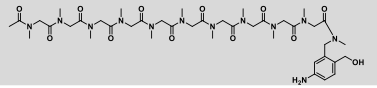	T1000	-7.531

Supplementary Figure S5. Physicochemical and functional equivalence of Tras-GGFG-DXd and DS-8201a.

A. SEC/HIC of DS-8201a (red) and internally synthesized Tras-GGFG-DXd (blue). Two ADCs showed identical profile (overlapping red and blue color).

B. Identical mass spectroscopy detection of DS-8201a and Tras-GGFG-DXd. All ADCs were predigested with PNGaseF to remove the N-glycans to yield the deglycosylated ADC before LC-MS acquirement. The LC-ESI-MS analysis of the light chains (LCs) and heavy chains (HCs) showed that the shifts of molecular weight were consistent with the attached linker payloads and high homogeneity of the all ADCs.

C-E. Functional equivalence of Tras-GGFG-DXd to DS-8201a was validated in vivo. ADCs were intravenously administered (indicated by a red arrow and doses were indicated on the graph) when tumor size reached an average of 150-200 mm^3. Each value represents the mean and SEM (n=5). Tumor growth inhibition rate in both models was almost identical for Tras-GGFG-DXd (blue) and DS-8201a (red). Tras-GGFG-DXd/DS-8201a was more effective in HCC1954 (medium to high HER2 expression) than in COLO205 or JIMT-1 (low HER2 expression).

F. Pharmacokinetics of total antibody and ADC after a single iv administration of ADC at 10 mg/kg or 3 mg/kg in mice (n=3, mean±SD). Total antibody and ADC was measured by method depicted in Supplementary Fig.S8B, S8C.

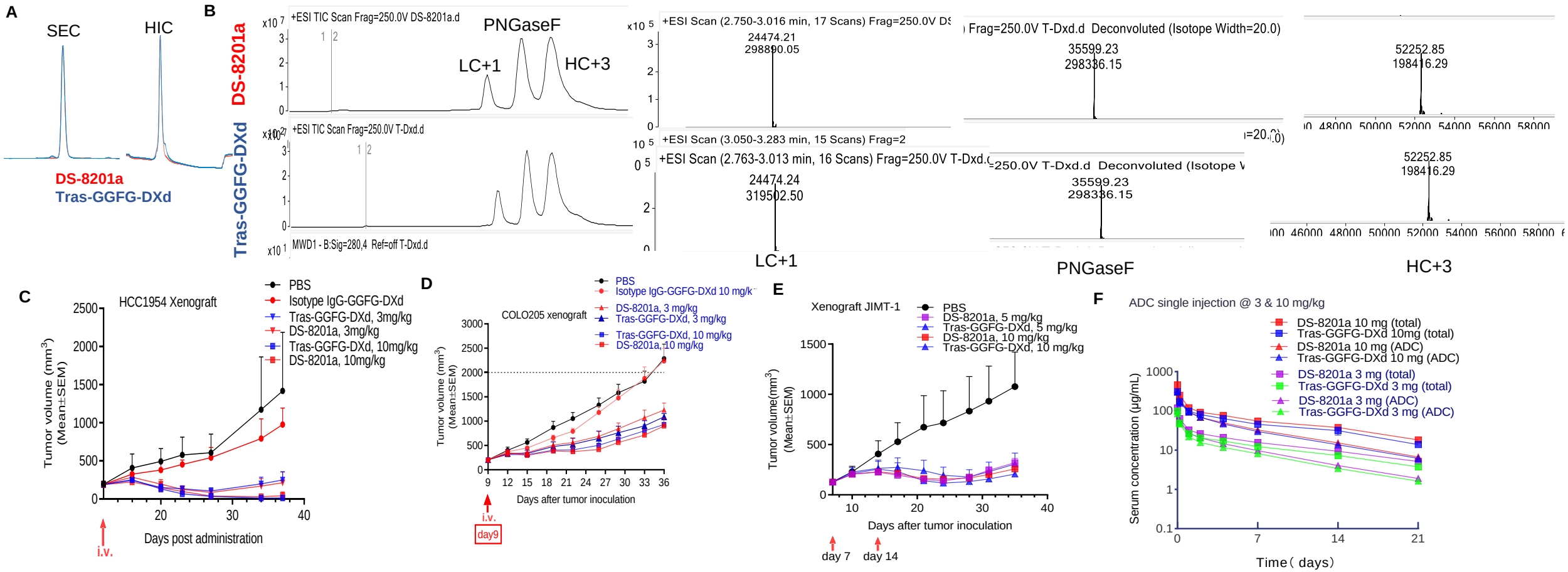

Supplementary Figure S6. Physicochemical profile of antibody-exatecan conjugates enabled by T moiety.

A. Antigen (recombinant HER2 protein) binding of MTX-1000, Trastuzumab (Tras) and Tras-GGFG-DXd measured by ELISA. Representative data from n=2 measurements, each performed in triplicates.

B. Flow cytometry of MTX-1000, Trastuzumab (Tras) and Tras-GGFG-DXd binding to COLO205 relative to an isotype control antibody (IgG).

C. Size Exclusion Chromatograms (SEC) of T moiety-exatecan ADCs targeting HER2 using Trastuzumab (Tras). Tras-GGFG-DXd is included. High aggregation was seen in a conjugation using unmodified PABC (Tras-PABC-exatecan) directly with antibody.

D. Hydrophobic Interaction Chromatograms (HIC) of T moiety-exatecan ADCs compared to naked antibody (T). ADC is labeled from highest to lowest hydrophilicity: Tras-exatecan ADCs were all more hydrophilic than Tras-GGFG-DXd.

E. Tras-T1000-exatecan/MTX-1000 with DAR 8 and DAR 4 by the reverse-phase chromatographic analysis.

F. ADC stability comparison. Stability of T moiety-exatecan ADCs, Tras-GGFG-DXd and Trastuzumab (Tras) was charactered by HPLC at 37^{0}C (7 days) and under a freeze-thaw condition (-80^{0}C for 30 minutes then room temperature to thaw, 3 repeats).

G,H. Thermostability and photostability of T-moiety ADCs and DS-8201a. ADC aggregation was analyzed by SEC (Size Exclusion Chromatography) after heating under 55^{o}C (G) or placed under the lab light (300-500 Lux) (H) for 72 hours.

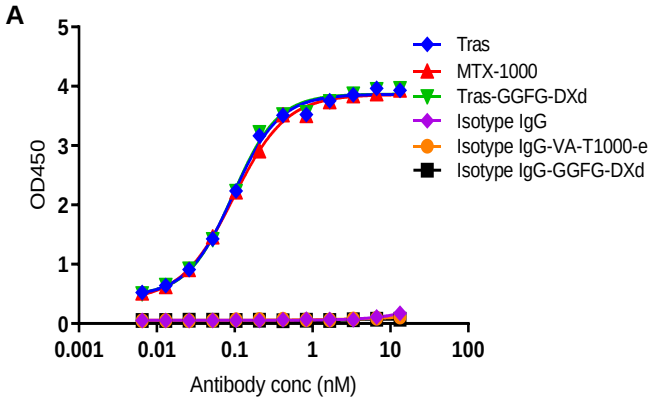

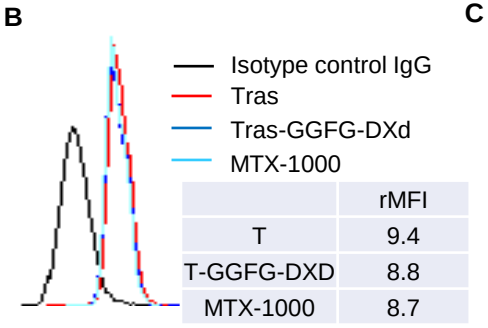

	rMFI
T	9.4
T-GGFG-DXD	8.8
MTX-1000	8.7

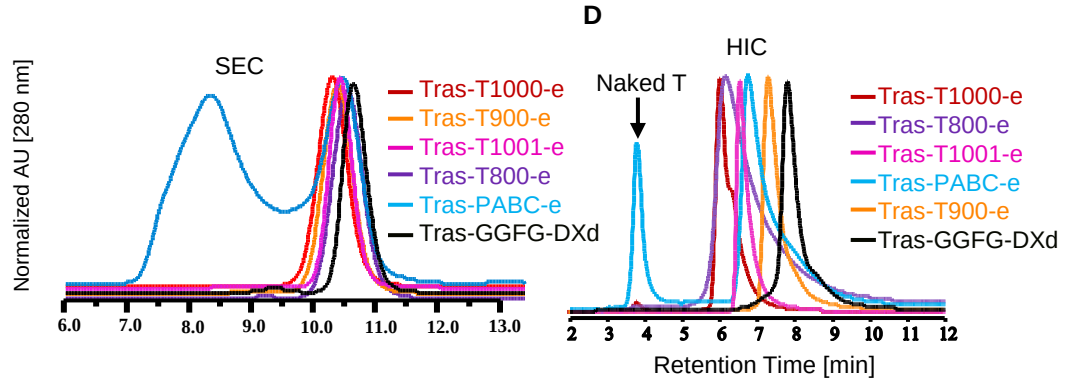

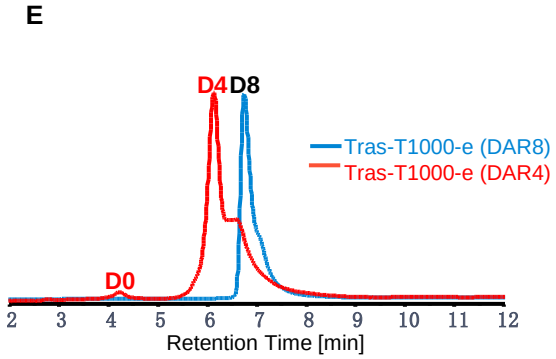

F

ADC aggregation	Freeze & Thaw	37°C-7d
T	0.24 %	0.26 %
Tras-T1000-e	0.79 %	1.16 %
Tras-T1001-e	1.75 %	4.08 %
Tras-T800-e	5.55 %	7.4 %
Tras-T900-e	1.91 %	5.83 %
Tras-GGFG-DXd	2.81 %	5.71 %

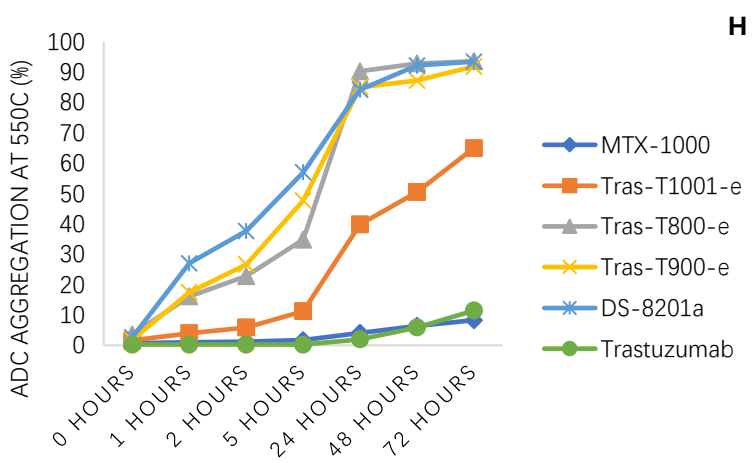

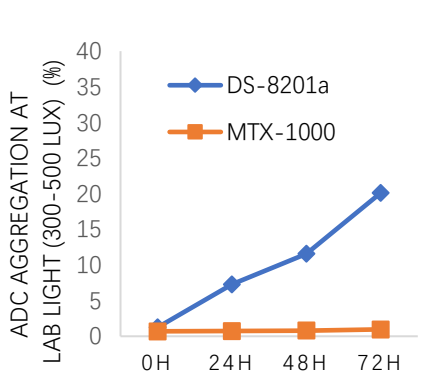

Supplementary Figure S7. Additional T moiety-exatecan and belotecan conjugates.

A-C. T moiety-exatecan conjugates for HER3 (A), TROP2 (B) and CDH6 (C). Antibody Patritumab for HER3, Datopotamab and hRS7 (IMMU-132) for TROP2 and DS6000 for CDH6 was used. HIC and SEC data was shown. TROP2 ADC is DAR 4 and hRS7-T1000-exatecan was also referred as MTX-132 in this study.

D. Chemical structure of belotecan.

E. T moiety-belotecan conjugate using HER2-targeting antibody Trastuzmab. HIC and SEC data was shown

F. Cytotoxicity of belotecan and its ADC Tras-T1000-belotecan in HER2+ (N87) and HER2- (MDA-MB-468) cell line.

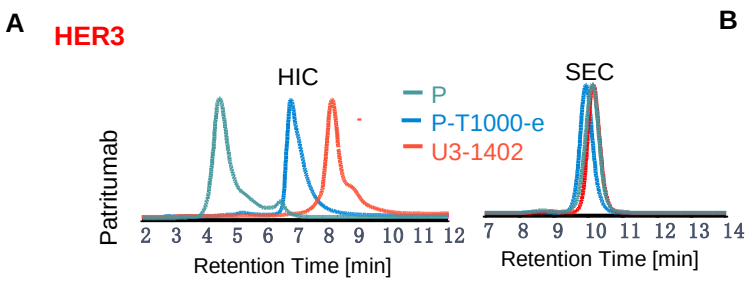

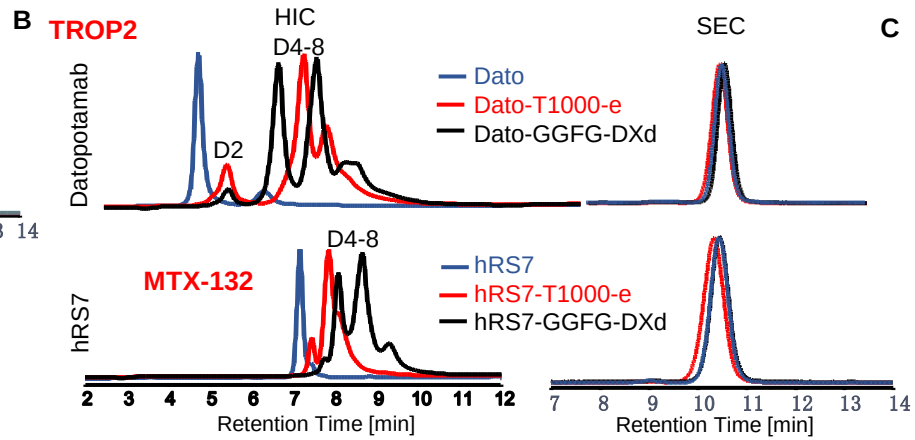

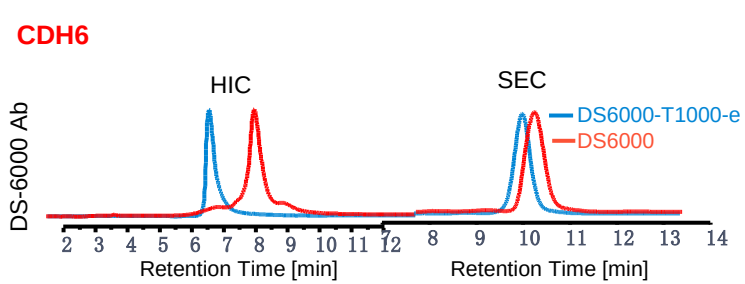

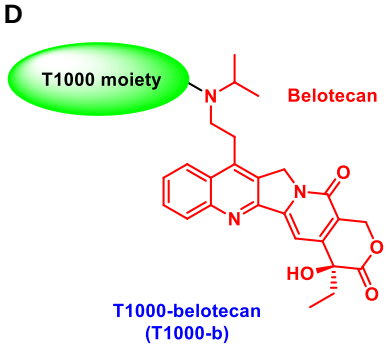

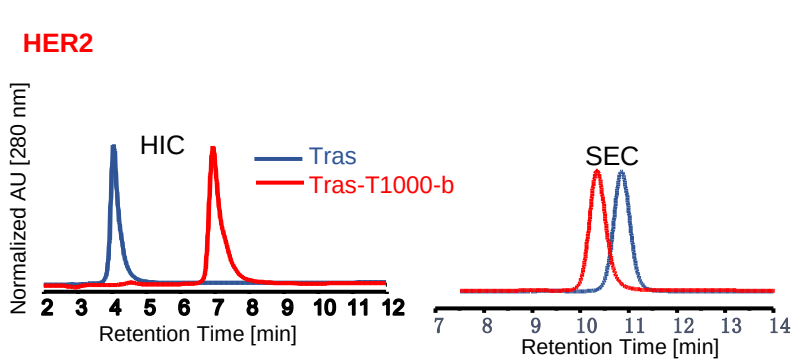

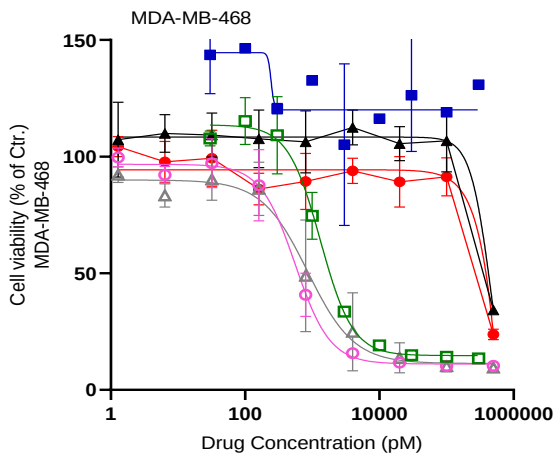

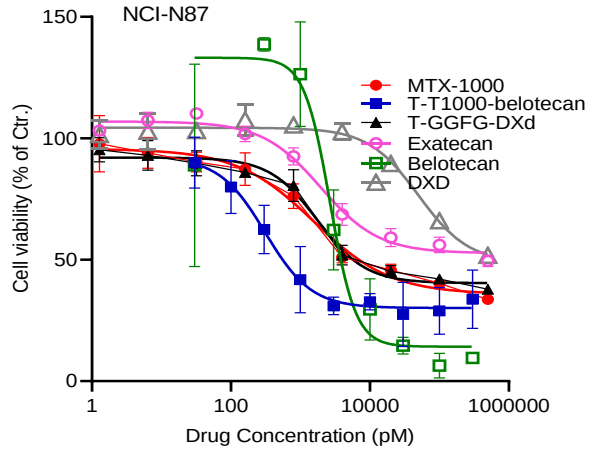

Cell Line	IC_{50} (nM)					
	Exatecan	DXD	Belotecan	MTX-1000	Tras-GGFG-DXd	Tras-T1000-Belotecan
NCI-N87	2.1	8.2	2.7	1.6	1.8	0.3
MDA-MB-468	0.6	0.9	1	inactive	inactive	inactive

Supplementary Figure S8. In vitro and in vivo stability of MTX-1000.

A. In vitro stability of Tras-T1000-exatecan/MTX-1000 in plasma measured by toxin release compared to that of Tras-GGFG-DXd.

B,C. Total antibody or ADC in vitro plasma stability of MTX-1000 compared to Tras-GGFG-DXd. 1mg/ml of ADC was diluted in human, monkey, mouse and rat plasma and measured by ELISA (assay format is shown below).

D. Comparison of payload release of ADC in rat measured by LC-MS at indicated time point.

E. Pharmacokinetic parameters of total antibody and ADC after a single iv administration of ADC at 4 mg/kg in rats (n=3, mean±SD).

A

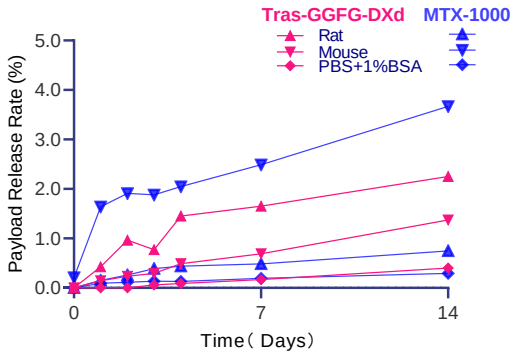

B

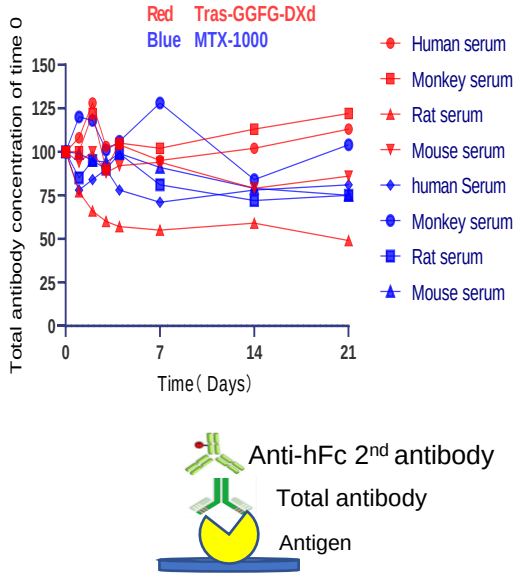

C

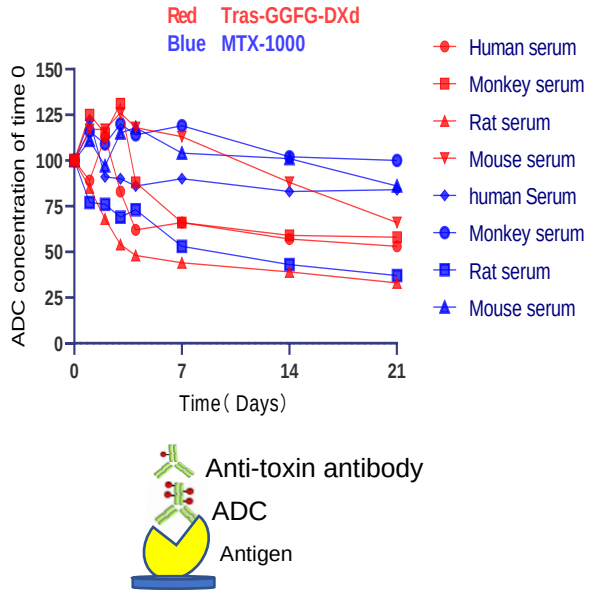

D

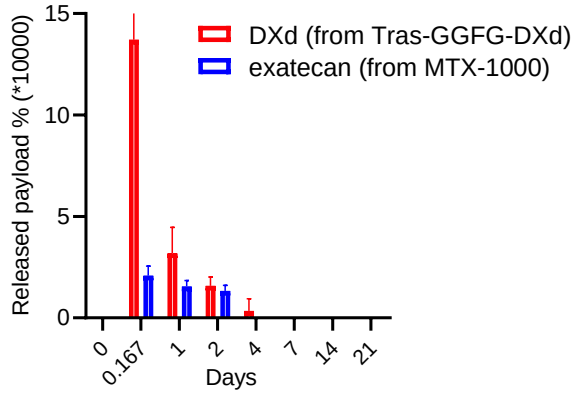

E

Pharmacokinetic parameters of total antibody and ADC after a single iv administration of ADC at 4 mg/kg in rats (N=3, mean±SD)					
	AUC	T1/2	Cmax	Vss	CL
	μg*day/mL	Day	μg/ml	mL/kg	mL/day/kg
Tras-GGFG-DXd (Total antibody)	288±31	6.35±2.25	79±7.0	NA[a]	NA[a]
Tras-GGFG-DXd (ADC)	213±41	4.14±1.45	73±10	110.3±37	18.7±4
MTX-1000 (Total antibody)	495±52	9.8±0.7	77±5	NA[a]	NA[a]
MTX-1000 (ADC)	319±79	7.4±1.5	78±16	168.9±12.1	19.6±3

Supplementary Figure S9. Cellular dynamics and mechanism of MTX-1000.

A. HER2 expression on different cell lines by flow cytometry. Expression is classified as High, Medium and Low for MFI of HER2 antibody (T) relative to an isotype control antibody (IgG) is >100, 20-100 or <20, respectively.
B. Internalization rate of MTX-1000 (T) and Tras-GGFG-DXd (D) on cancer cell lines measured by flow cytometry.
C. Internalization rate of MTX-1000 and Tras-GGFG-DXd on cancer cell lines at 8 hours after ADC binding measured by flow cytometry.
D. No correlation of DXd release and target expression. HER2 expression on each cell line is determined by flow cytometry and DXd concentration in the culture media at 24 hours after treatment with 100 nM DS-8201a was determined by LC/MS-MS (n=3)
E. DS-8201a was less stable in cell culture media than MTX-1000. ADCs were incubated with cell culture media with 10% FBS for 8 and 24 hours. Released payload was detected LC/MS-MS (n=2). Top graph showed the released payload concentration ratio of DS-8201a/MTX-1000 and bottom table showed concentration measurements.
F. Detection of DNA-trapped TOP1 by MTX-1000 and DS-8201a. Left panel, COLO205 cells were treated with the indicated drug concentrations for 30 minutes. TOP1ccs were isolated by RADAR assay. The intensity of TOP1 was analyzed by ImageJ software and normalized to DNA loading (right panel). Data were plotted with GraphPad Prism 8. Quantitation of TOP1ccs was in Fig.2E.
G. TOP1 degradation induced by exatecan. COLO205 cells were incubated with the indicated TOP1 inhibitors for 2 hours. Following TOP1 reversal for 30 minutes without inhibitors, TOP1 levels were determined by Western blotting. D, Quantification of total cellular TOP1 bands in duplicate experiments. Band intensity was analyzed using the ImageJ software and normalized to GAPDH used as a loading control. Result tabulation in Fig.2F.
H. DNA damage induction and apoptosis. HCC1954 cells treated with MTX-1000 or controls for up to 72 hours were analyzed by Western blot for DNA damage (γH2AX, pKAP1 and pChk1) and apoptosis (cleaved PARP) markers.

A

Cell Line	Cancer Type	HER2 Expression	
		Relative MFI (HER2/Isotype IgG)	(High-Medium-Low)
NCI-N87	Stomach	421	High
HCC1954	Breast	85	Medium
T-47D	Breast	16	Low
MDA-MB-468	Breast	1	NO
H2170	Lung	180	High
HCT-15	Colon	12	low
COLO205	Colon	9	Low
SKOV-3	Ovary	120	High
SW620	Colon	3	Low

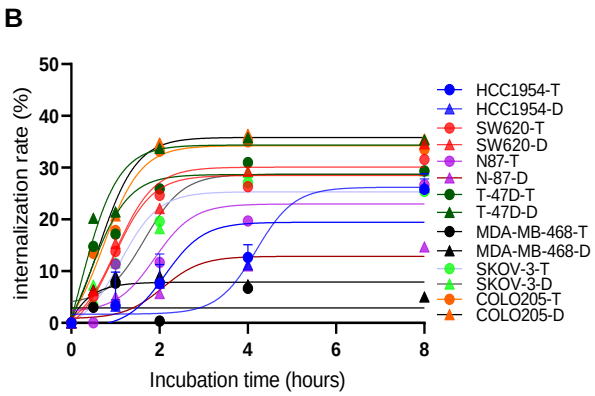

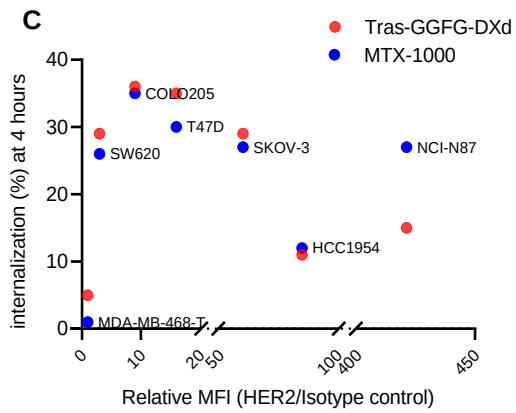

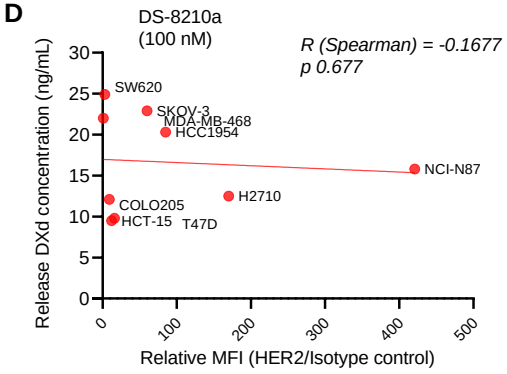

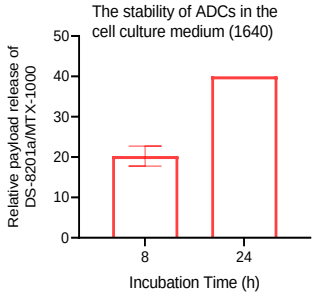

ADC	Incubation time (hours)	Payload concentration (ng/ml)		Average
DS-8201a	0	Below detection		
	8	1.85	1.99	1.92
	24	4.88	5.20	5.04
MTX-1000	0	Below detection		
	8	0.09	0.09	0.09
	24	0.12	0.13	0.13

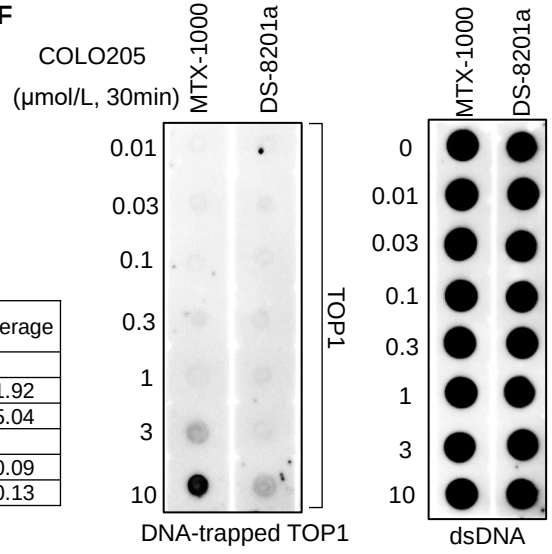

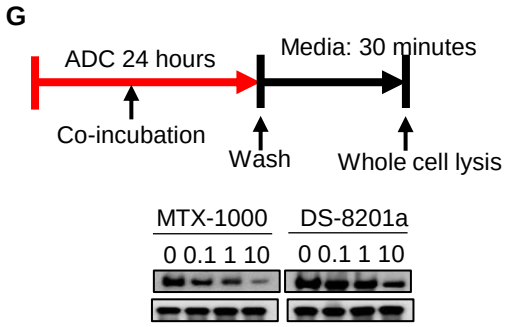

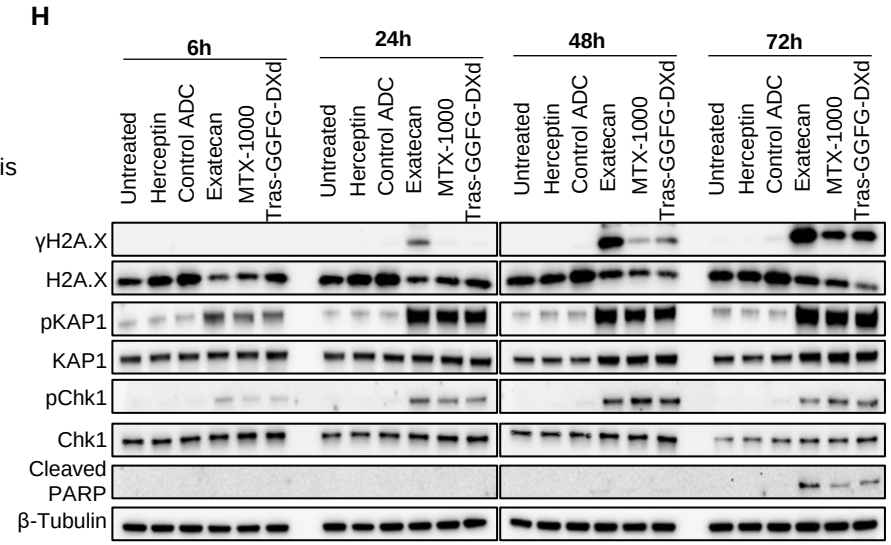

Supplementary Figure S10. Colon cancer organoid response to ADCs.

A. Representative IHC of HER2 expression in a patient sample used to derive a colon cancer organoid (P6).

B. Representative H&E staining of colon cancer organoid P6. Full view and enlarged individual organoids were shown. Scale bar was labeled.

C,D. Representative images of live/dead cells of organoid P6 at Day 0 (C) before the administration of indicated ADC and Day 6 (D) after the drug treatment. Left, whole view of a 96-well. Right, enlarged view of a selective section. whole Colon cancer PDO cells were stained by Calcein AM (green) and dead cells by PropidiumIodide (PI) (red). Scare bars were shown.

E. (P6) Organoid dose-response to ADC after 6 days of drug treatment. Surviving organoids data shown are means ± SE from two independent experiments.

F. Schematic depiction of measuring ADC penetration into an organoid. An organoid was artificially divided into four (4) circles of areas from Surface to Core. Live or dead cells in each circular area was counted and used to plot live/dead cell distribution (Supplementary Fig.10F; Fig.2I).

G. Quantification of ADC penetration of organoid. Spatial distribution of Calcein AM staining signal of MTX-1000 versus DS-8201a from the organoid Surface to Core.

H. A PDO response to MTX-1000 and DS-8201a after 6 days. Representative images of brightfield (left) and live/dead cells (right) for an organoid were shown. Colon cancer PDO was treated with MTX-1000 or DS-8201a at a concentration of 50 ug/ml. Live cells were stained by Calcein AM (green) and dead cells by PropidiumIodide (PI) (red). Scar bar was shown.

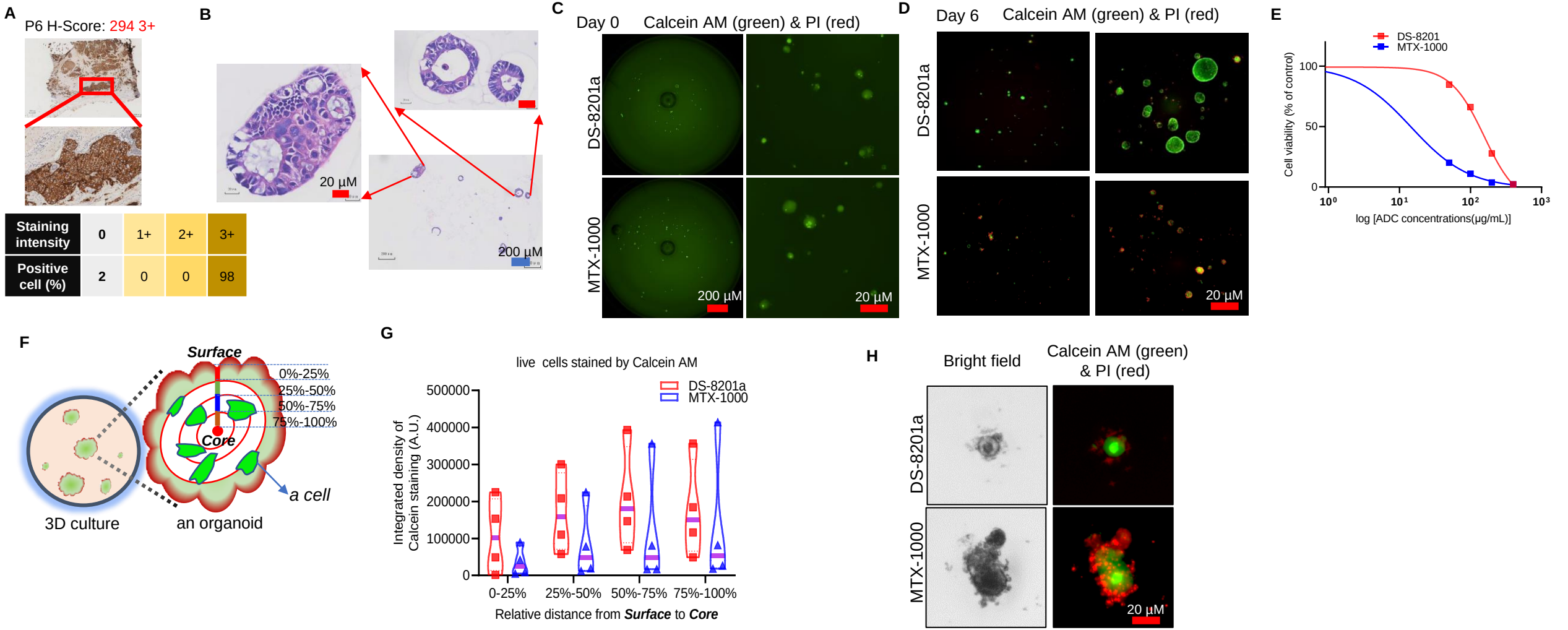

Supplementary Figure S11. Bystander killing effect of MTX-1000, T-DM1 and Tras-GGFG-DXd in coculture conditions *in vitro*.

A, B. Growth inhibitory activity of ADCs against HCC1954 (HER2+) and MDA-MB-468 (HER2-) cells. Tumor cells were treated with ADCs for 5 days and cell viability (%) was calculated. Each point represents the mean and SD (*n* = 3).

C. Data of flow cytometric analysis. HCC1954 and MDA-MB-468 cells were cocultured and treated with 10 nM ADCs for 5 days. After collecting adherent cells, cell number and ratio of human epidermal growth factor receptor 2 (HER2)-positive and HER2-negative cells were determined by a cell counter and a flow cytometer, respectively.

D. Numbers of HCC1954 and MDA-MB-468 viable cells (mean, n= 3).

A

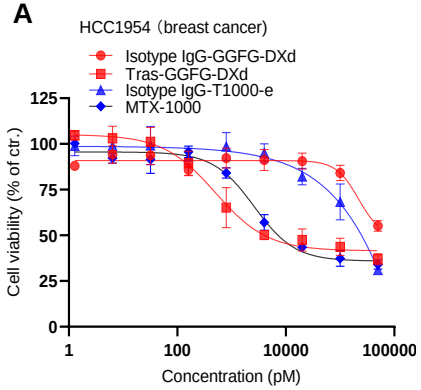

B

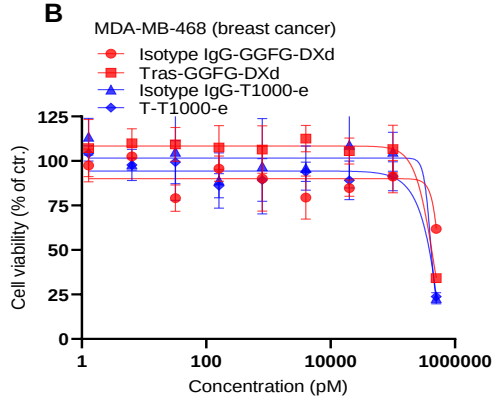

C

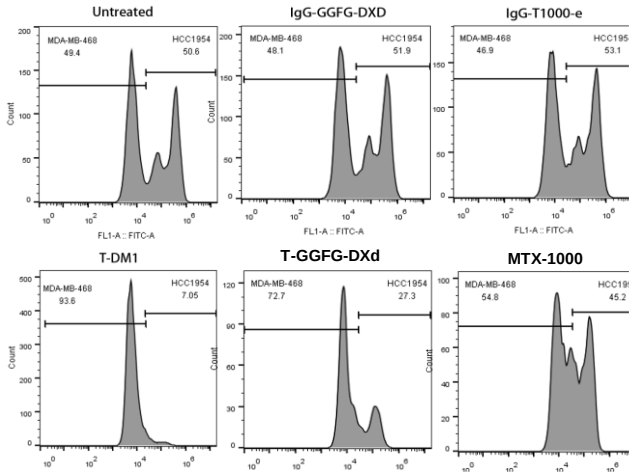

D

	Cell Number（Mean）	
	HCC1954 ($x10^4$)	MDA-MB-468 ($x10^4$)
Untreated	27.3	26.7
T-DM1	2.6	37.4
Isotype IgG-GGFG-DXD	23.9	22.1
Tras-GGFG-DXd	**3.3**	**8.7**
Isotype IgG-T1000-exatecan	23.9	21.1
Tras-T1000-exatecan (MTX-1000)	**3.39**	**4.11**

Supplementary Figure S12. Hematology and serum chemistry of MTX-1000 in monkey

Six monkeys were given vechicle, 10, 30 mg/kg MTX-1000 on day 1, 22, 43 (shown as arrows) and with a 1-week recovery period.

A. Body weight change. Dashed line indicates starting body weight.

B-G. Hematology. Count of white blood cells. G. Count of neutrophils. MTX-1000 toxicity in cynomolgus monkeys (cross-reactive species) was conducted by a repeated intravenous dosing (every 3 weeks for 3 doses at 10 mg/kg and 30 mg/kg) study. ADC was given at the indicated.

H, I. Serum chemistry.

J. Summary of major toxicity findings of MTX-1000 compared to Tras-GGFG-DXd.

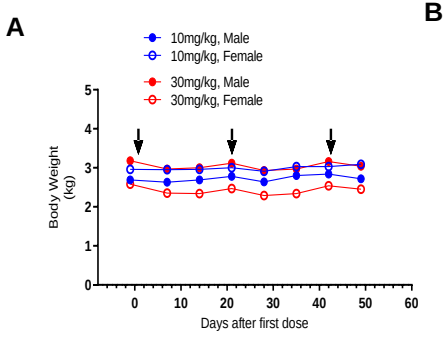

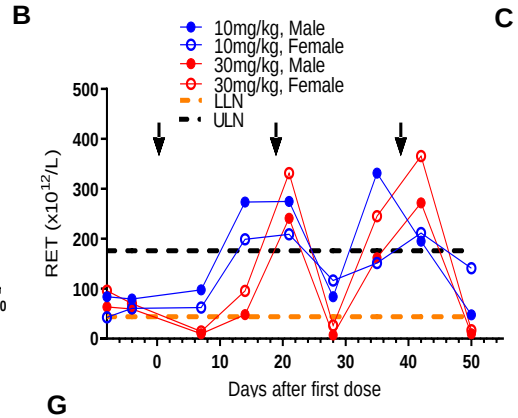

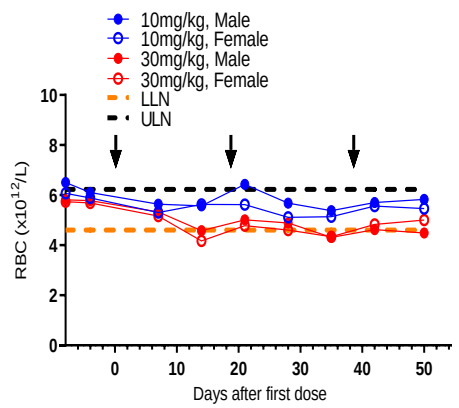

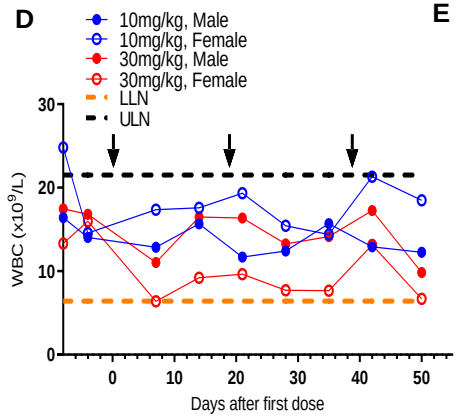

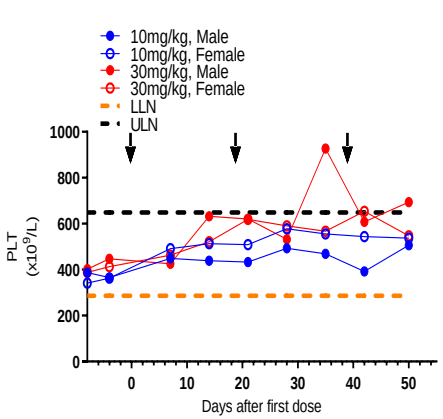

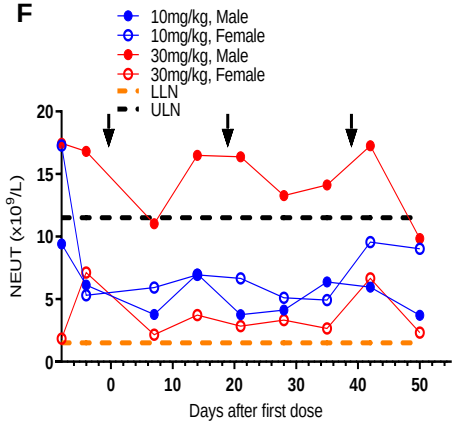

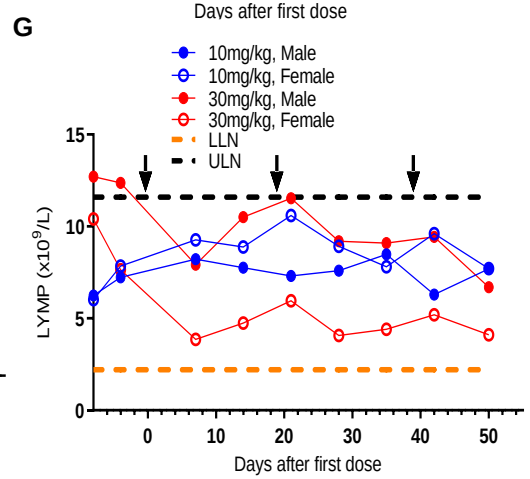

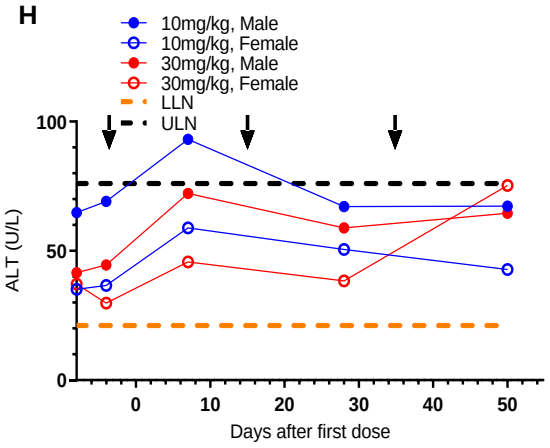

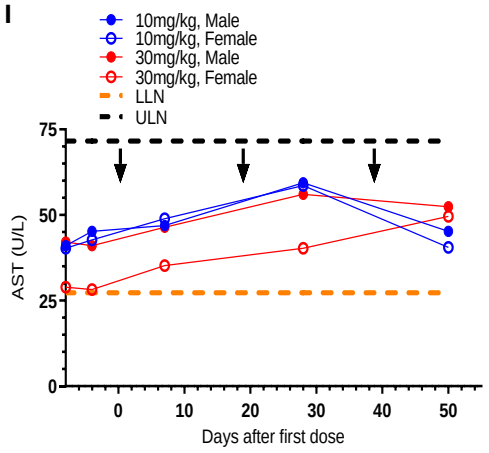

J

Compound	MTX-1000		T-GGFG-DXd (SBL315-031)		T-GGFG-DXd (SBL315-553)	
Species	Cynomolgus monkey					
Regimen	Q3W*3					
Dose(mg/kg)	10	30	10	30	10	30
Dead/moribund	0	0	0	0	0	0
Clinical signs	-	-	-	-	-	-
BW/FC	-	-	-	-	-	-
Hematology	-	RET↓	-	-	-	RBC↓
Serum chemistry	-	-	ALT↑, AST↑	ALT↑, AST↑	AST↑, LDH↑, CREA↑	AST↑,LDH↑, CREA↑
Gross Pathology	-	small-sized thymuses	-	-	-	-
Histopathology	-	lymphocyte moderate reduction	intestines	lung, skin, testis	intestines	Skin injection sites, bone marrow (decreased erythroblasts)

Supplementary Figure S13. T moiety-exatecan ADCs show potent antitumor efficacy and improved therapeutic index

A-D. In vitro cytotoxicity of T moiety-exatecan ADCs against cancer cell lines. Cells were treated at a concentration series of ADCs for 6 days and IC_{50} of each cell line was calculated. Inactive is shown as IC_{50} of > 100 nM or labeled as such if accurate IC_{50} can not be accurately determined. Representative data (mean and SD) from 2 or 3 measurements. A. HER2 expression (relative MFI) and MTX-1000 and Tras-GGFG-DXd cytotoxicity. B. MTX-1000/Tras-GGFG-DXd cytotoxicity with/without ABCG2 inhibitor Reserpine in H460. Flow cytometry of HER2 expression relative to isotype control IgG is shown on the left. C. TROP2-targeting ADC cytotoxicity. Datopotamab-T1000-exatecan and Datopotamab-GGFG-DXd with respective isotype control IgG ADC is compared in a low TROP2 expression cell LK-2. Flow cytometry of target expression is shown on the left. D. HER3-targeting ADC cytotoxicity. Patritumab-T1000-exatecan and Patritumab-GGFG-DXd with respective isotype control IgG ADC is compared in a low HER3 expression cell COLO205. Flow cytometry and IHC data of target expression is shown on the left. Scale bars, 50 µm.

E. In vivo efficacy of MTX-1000 (blue) and Tras-GGFG-DXd (red) in a HER2 high expression xenograft (CDX) model. HER2 expression is shown on the left as flow cytometry (relative MFI) and IHC image on untreated mouse tumor tissue and H-score. Scale bars, 50 µm. CDX mice were intravenously administered with indicated ADCs (10 mg/kg) on day 0 (tumor size reached about 200 mm^3) and 7 (red arrows). Each value represents the mean and SEM (n=5). Body weight change of each animal group is shown on the right.

F. In vivo efficacy of TROP2-targeting ADCs. MTX-132 (blue) and Trodelvy (purple) and Dato-GGFG-DXd (red) in a TROP2 high expression xenograft (CDX) model.

G. In vivo efficacy of TROP2-targeting ADCs. MTX-132 (blue) and Trodelvy (red) in a TROP2 medium expression xenograft (CDX) model.

H. Summary of therapeutic index estimation based on monkey HNSTD and minimum efficacious dose (MED) for tumor regression. Data was based on published results and from this study.

I. Pharmacokinetics of total antibody and ADC after a single iv administration of ADC at 10 mg/kg or 3 mg/kg in mice (n=3, mean±SD). Data from Supplementary Fig.S5F.

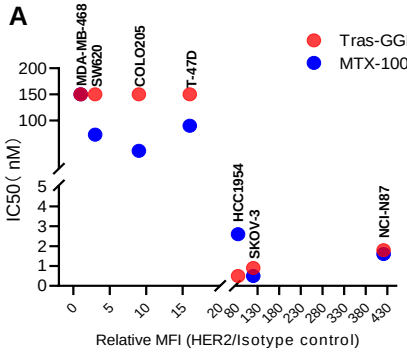

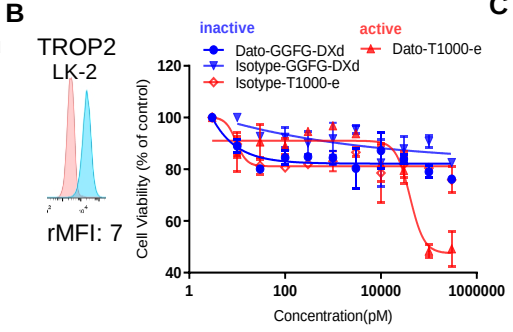

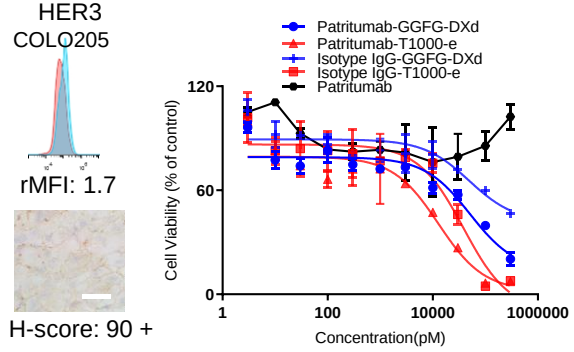

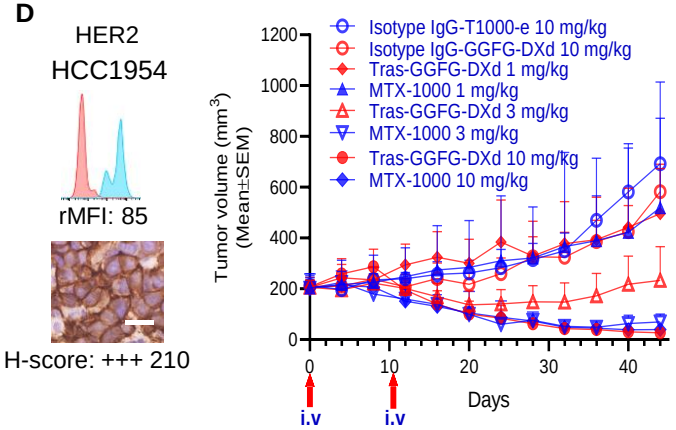

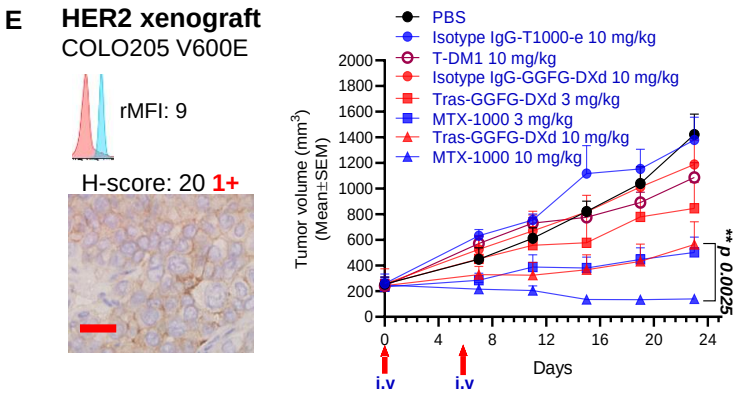

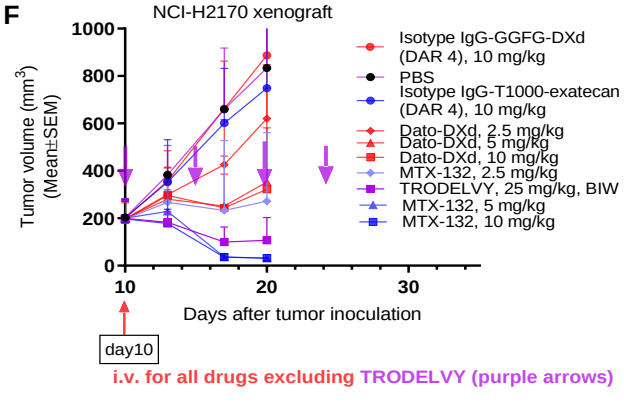

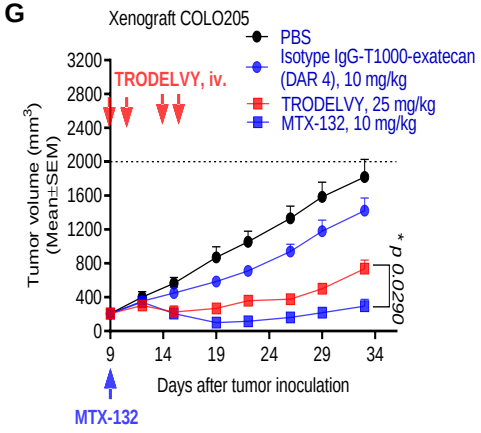

H

Therapeutic Index	*Toxicity profile*		*Minimum efficacious dose (MED) for tumor regression*		*Mouse PK (AUC)* µg*day/mL		Therapeutic Index	
	HNSTD (mg/kg)	AUC µg*day/mL	Medium-High target expression tumors	Low target expression tumors	3 mg/kg	10 mg/kg	Monkey HNSTD*4/ MED[b]	AUC ratio[a]
HER2								
DS-8201a	30	3930[e]	10 mg/kg	Not effective		736	12	5.3
MTX-1000	30	2705	3 mg/kg	10 mg/kg	271		40	10
TROP2								
Dato-GGFG-DXd	10[c]	Not applicable	>10 mg/kg	Not effective	Not applicable		4	Not applicable
Dato-T1000-exatecan	30		5 mg/kg	10 mg/kg			24	
IMMU-132	50[d]		25 mg/kg	25 mg/kg			8	
MTX-132	30		3 mg/kg	10 mg/kg			40	

I

Pharmacokinetic parameters of total antibody and ADC after a single iv administration of ADC at 3 mg/kg and 10 mg/kg in non-tumor bearing mice (n=3, mean±SD)

ADC dose	3 mg/kg		10 mg/kg	
	AUC µg*day/mL	T1/2 Day	AUC µg*day/mL	T1/2 Day
DS-8201a (Total antibody)	326±17	8.6±0.8	1209±24	8.6±0.9
DS-8201a (ADC)	212±10	5.8±0.4	736±31	5.8±0.5
MTX-1000 (Total antibody)	343±2	9.7±0.4	1171±69	7.5±0.5
MTX-1000 (ADC)	271±3	7.3±0.6	1032±36	8±0.4

a. The ratio of ADC exposure (AUC) associated with HNSTD divided by that associated with minimum efficacious dose (MED) to cause tumor regression. See References. Junutula, J. R. et al. Clin. Cancer Res. **16**, 4769-4778 (2010); Muller, P. Y. & Milton, M. N. Nature Rev.. Drug Discovery **11**, 751-761 (2012)

b. The ratio of monkey HNSTD and minimum efficacious dose (MED) scaled according to body surface area (HNSTD*4/MED to cause tumor regression)

c. D. Okajima et al., Datopotamab Deruxtecan, a Novel TROP2-directed Antibody-drug Conjugate, Demonstrates Potent Antitumor Activity by Efficient Drug Delivery to Tumor Cells. Molecular cancer therapeutics **20**, 2329-2340 (2021)

d. https://www.accessdata.fda.gov/drugsatfda_docs/nda/2020/761115Orig1s000MultidisciplineR.pdf

e. Xenobiotica; the fate of foreign compounds in biological systems **49**, 1086-1096 (2019).

Supplementary Figure S14. T moiety-exatecan ADCs show higher antitumor potency in PDX models and better intratumor pharmacodynamic response.

A-F. In vivo efficacy of T moiety-exatecan (blue) and GGFG-DXd (red) ADCs in PDX models. Target and PDX tumor type is labeled. Target expression in each model is shown as IHC image on untreated mouse tumor tissue and H-score. Scale bars, 20 µm. PDX mice were intravenously administered with indicated ADCs (10 mg/kg) and on day 0 (tumor size reached an average of 150-200 mm^3) and subsequent dates indicated by red arrows. Each value represents the mean and SEM (n=4 or 5). Unpaired two-sided t-test. *P<0.05, **P<0.01, ***P<0.001. ADCs used for each model: A, D and F, HER2-targeting MTX-1000 and/or MTX-800 and Tras-GGFG-DXd. B, C and E, TROP2-targeting Dato-GGFG-DXd and hRS7-T1000-exatecan (MTX-132).

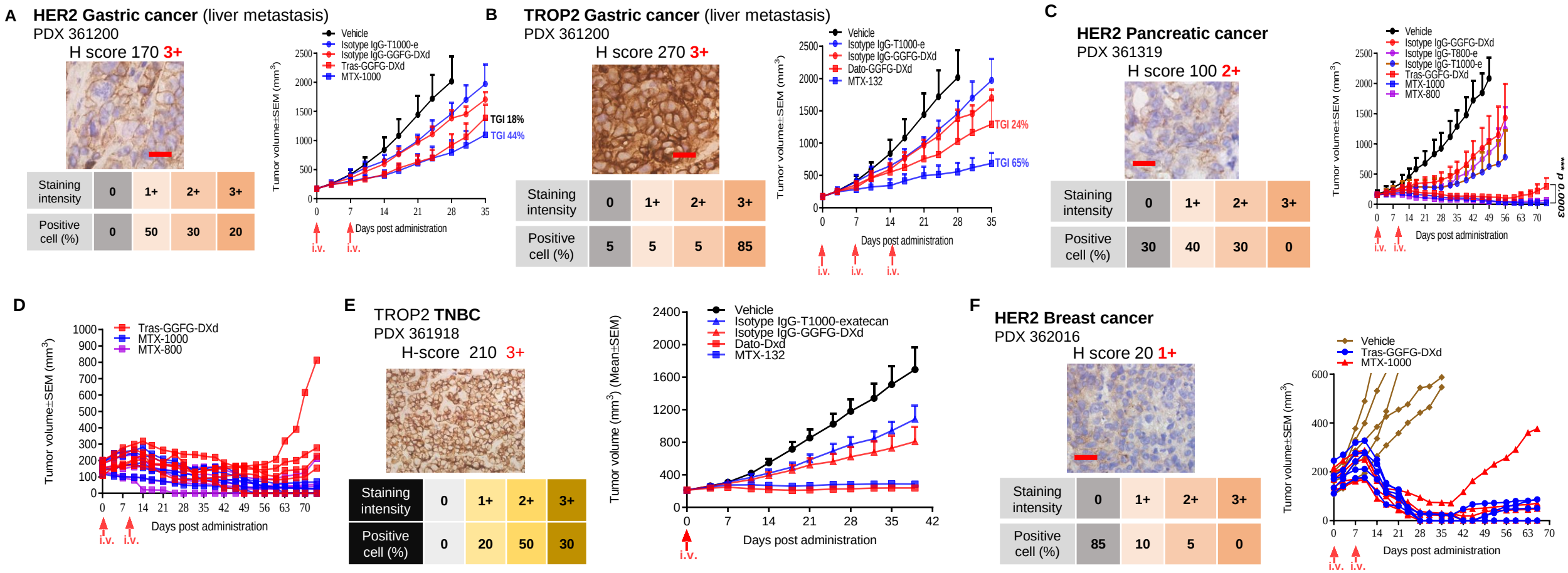

Supplementary Figure S15. T moiety-exatecan ADCs overcome treatment-resistance due to improved therapeutic index and intratumor pharmacodynamic response.

A. MTX-1000 overcame DS-8201a-treatment resistant tumor in HCT-15 xenograft model. Experimental design and ADC dosing was shown.

B. MTX-132 overcame Trodelvy treatment-resistant tumor in COLO205 xenograft model. Two tumor size groups (800 or 1500 mm^3) were plotted individually from Fig.3E. MTX-132 caused tumor regression comparing to continuing tumor growth in the Trodelvy group. ADC dose was labeled.

C,D. MTX-132 overcame Dato-DXd treatment-resistant tumor in H2170 (C) and HCT-15 (D) xenograft model. . Experimental design and ADC dosing was shown for each model.

E. In vivo pharmacodynamics of MTX-1000 and DS-8201a. MTX-1000 and DS-8201a was administrated in COLO205 model. Tumor tissues were obtained after 24 and 72 hours for γH2AX IHC measurements.

F. Tumor size measurement for pharmacodynamic study in COLO205. Left showed average tumor size and right showed individual tumor size at day 1 (top) and day 3 (bottom). n=3.

G. H-score for γH2AX IHC. Each had 3 mice and two measurements.

H. In vivo efficacy of HER3-targeting ADCs in ASPC-1.

In all in vivo studies, CDX mice were intravenously administered with indicated ADCs (at 10 mg/kg or at an indicated dose) on days indicated by an arrows. Each value represents the mean and SEM (n=5 or otherwise indicated). Unpaired two-sided t-test. *P<0.05, **P<0.01, ***P<0.001.

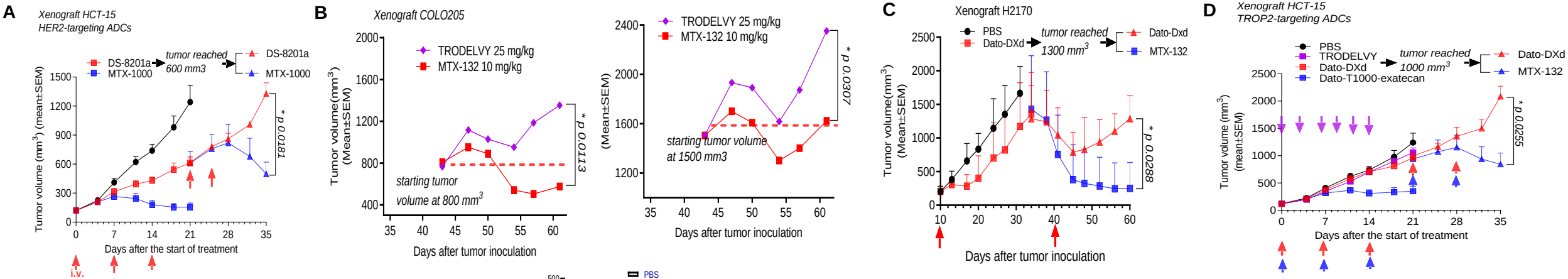

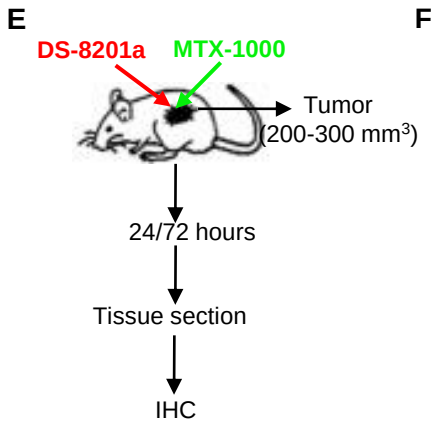

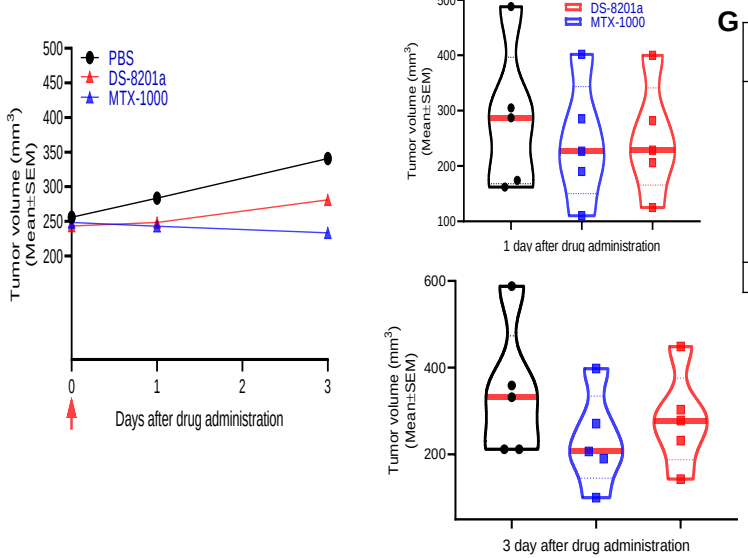

G

Group	Vehicle	MTX-1000 Day 1	MTX-1000 Day 3	DS-8201a Day 1	DS-8201 Day 3
H-Score	14.0	93.3	108.3	67.0	94.0
	13.0	98.3	85.0	81.3	61.7
	13.0	60.0	128.3	47.7	71.7
	13.0	88.3	93.3	64.3	90.0
	17.0	103.3	70.3	52.7	56.7
	33.0	53.7	100.0	38.3	73.3
Average	**17.2**	**82.8**	**97.6**	**58.6**	**74.6**

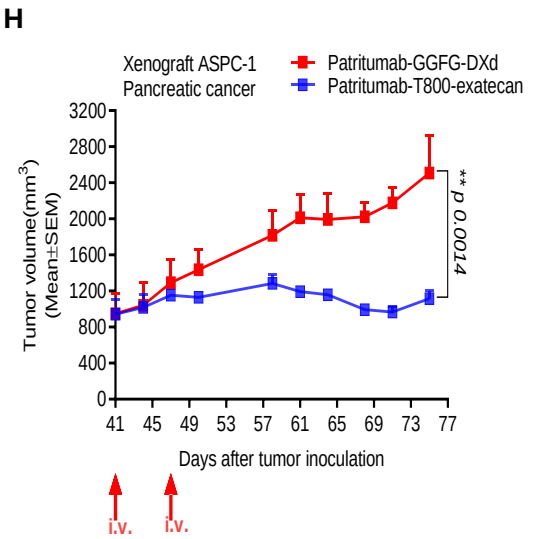

Supplementary Figure S16. Overcoming MDR resistance by T moiety exatecan ADCs or a combination of MDR inhibitor with DXd/SN-38 ADCs.

A. ABCG2/p-gp and target expression of cell lines for in vivo assays. ABCG2 is expressed in H2170 and ASPC1 while p-gp has a high expression in HCT-15 (shown as light green). HER2, HER3 and TROP2 expression level by flow cytometry is shown.

B-D, The improvement of in vitro cytotoxicity IC_{50} by MDR inhibition. Data shown was IC_{50} (nM) in the absence or presence of MDR inhibitor YHO-13351 against ABCG-2 (for H2170 and ASPC1) and Tariquidar against P-gp (HCT-15). ADC for each target was individually listed.

E. HER3-targeting ADCs in HCT-15 with and without p-gp inhibitor Tariquidar. Left, Tumor growth and inhibition. Right, Best percentage change of initial tumor volume from left.

F. TROP2-targeting ADCs in a PDX model with high p-gp expression. TROP2 expression (IHC) and MDR gene (mRNA expression) was shown. MTX-132 was effective while Dato-DXd was not for tumor inhibition. Two mice from Dato-DXd group were used to test combination treatment with p-gp inhibitor Tariquidar when tumors reached 600 mm^3 (Fig.4H).

In all in vivo studies, CDX/PDX mice were intravenously administered with indicated ADCs (at 10 mg/kg or at an indicated dose) on days indicated by an arrows. Each value represents the mean and SEM (n=5 or otherwise indicated). Unpaired two-sided t-test. **P*<0.05, ***P*<0.01, ****P*<0.001. For small molecule inhibitor, the dose of YHO-13351 and Tariquidar was 50mg/kg (PO, QDx5Dx1) and 15mg/kg (PO, QDx5Dx3), respectively.

A

Model	MDR status		Target expression (relative MFI to an isotype IgG by flow cytometry)		
	ABCG2 (mRNA)	P-gp (mRNA)	HER3	HER2	TROP2
NCIH2170	4.6	0.7	2.5	220	31
ASPC1	5.8	0.06	2.4	6.8	1.6
HCT15	1.239	6.8	6.9	19	16

B

HER3-targeting ADC (Patritumab-conjugate (IC_{50}, nM)									
	Cell line	P-DXd	P-DXd+ YHO-13177	P-T1000-exatecan	P-T1000-exatecan+ YHO-13177	P-DXd	P-DXd+ Tariquidar	P-T1000-exatecan	P-T1000-exatecan+ Tariquidar
ABCG2 high	ASPC1	860	83	119	78	190	93	104	55
P-gp high	HCT-15					Not effective	74	203	158

C

TROP2-targeting ADC (IC_{50}, nM)		Dato-conjugate				hRS7-conjugate			
		Dato-Dxd	Dato-Dxd+ Tariquidar	Dato-T1000-exatecan	Dato-T1000-exatecan + Tariquidar	MTX-132	MTX-132+ Tariquidar	Trodelvy	Trodelvy + Tariquidar
P-gp high	HCT15	Not effective	86	920	2500	600	440	0.5	0.25

D

HER2-targeting ADC (IC_{50}, nM)									
	Cell line	DS-8201a	DS-8201a+ YHO-13177	MTX-1000	MTX-1000+ YHO-13177	DS-8201a	DS-8201a+ Tariquidar	MTX-1000	MTX-1000+ Tariquidar
ABCG2 high	SNU5	220	60	90	31				
	ASPC1	190	93	104	55				
P-gp high	HCT-15					1437	89	170	118

E

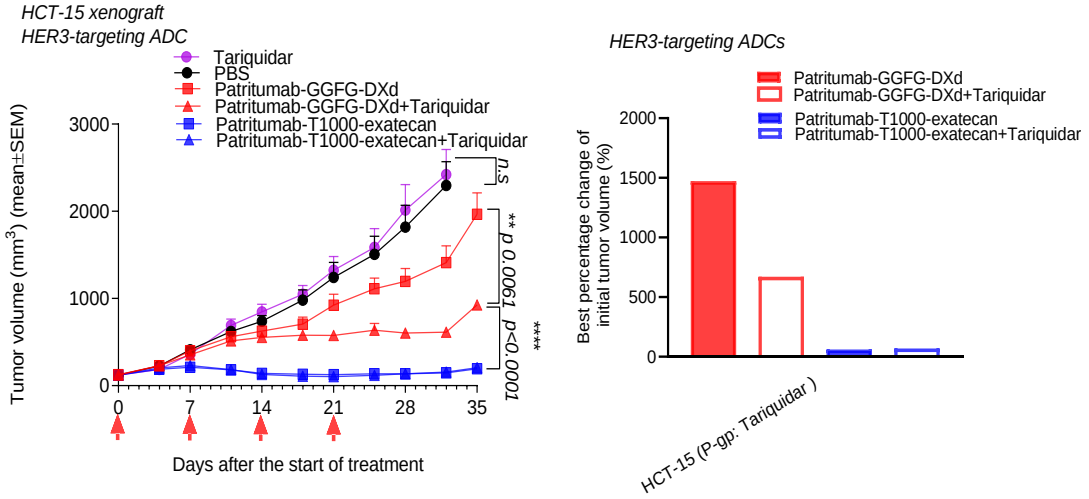

F

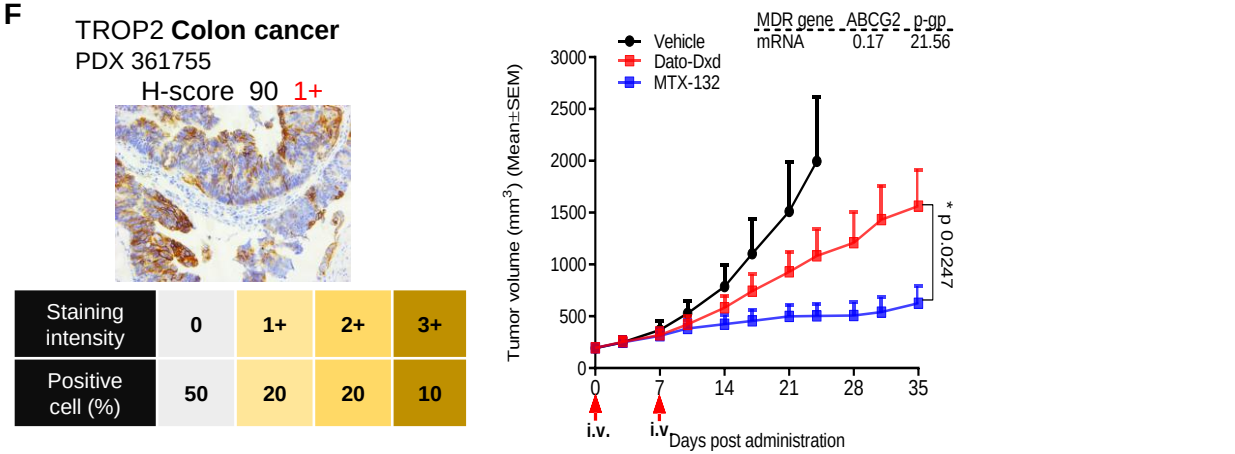

Supplementary Figure S17. Exatecan/MTX-1000 and PARP/ATR inhibitor synergize in colon cancer cells.

A-F. Cytotoxicity of exatecan and DXd with/without Tala (A,C,E) and M4344 (B,D,F) on COLO205. Cells were incubated with indicated drugs for 5 days. Data represent 2 independent measurements. IC_{50} was tabulated below each cytotoxicity curve. Cell viability curve(A, B). Tabulation of IC_{50} from A and B (C,D). E, F. Tabulation of IC_{50} improvement for exatecan/DXd with Tala (E) and M4344 (F).

G. Exatecan is more potent than DXd when synergized with Talazoparib and M4344. COLO205 cells were co-incubated with a concentration series of exatecan/DXd with Talazoparib (600 nM) or M4344 (25 nM) for 4 days (Supplementary Fig.S8A, 8D). IC_{50} of exatecan/DXd was calculated and shown as fold change. Data represent 2 independent measurements

H, I. Combination index (CI) of exatecan (blue line) or DXd (red line) with Tala (B) or M4344 (C) in COLO205. CI values <1 indicated synergism and were analyzed using the CompuSyn software (ComboSyn, Inc., Paramus, NJ, USA) with cell viability data of Supplementary Fig.S8A, 8D. Exatecan showed synergy with Tala and M4344 at lower concentrations than DXd (blue line on the left of the red line).

J. Cytotoxicity of MTX-1000 or Tras-GGFG-DXd on COLO205 with/without Tala and M4344. Cells were incubated with indicated drugs for 5 days. Data represent 2 independent measurements.

A

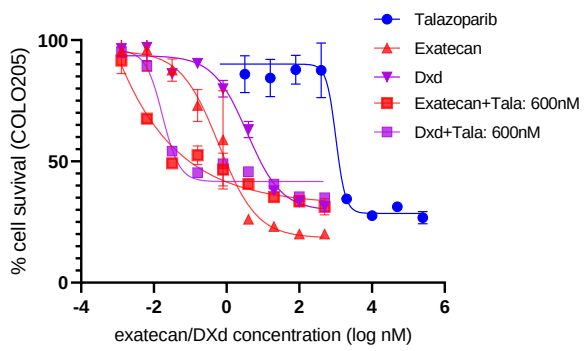

B

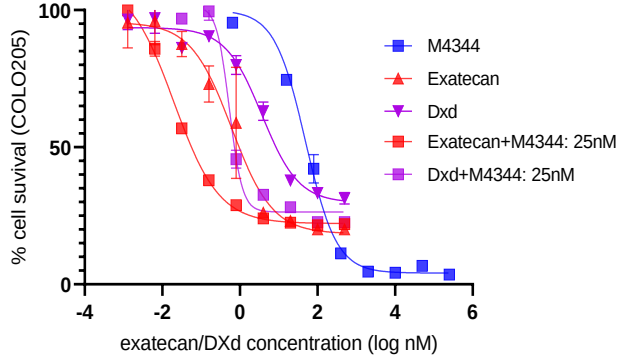

C IC_{50} (nM)

Exatecan	Dxd	Talazoparib	Exatecan+ Talazoparib (100nM)	Dxd+ Talazoparib (100nM)
0.3	3.7	1022	0.0013	0.02

D IC_{50} (nM)

Exatecan	Dxd	M4344	Exatecan+M4344 (15nM)	Dxd+M4344 (15nM)
0.3	3.7	49	0.02	0.53

E

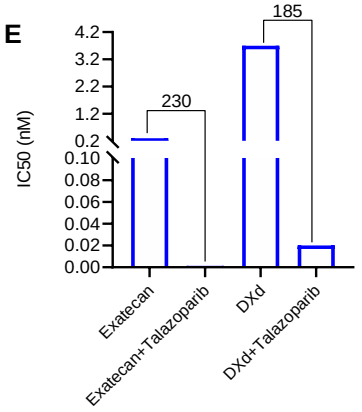

F

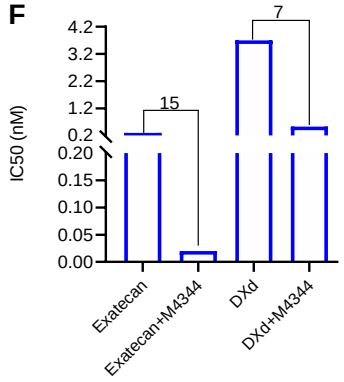

G

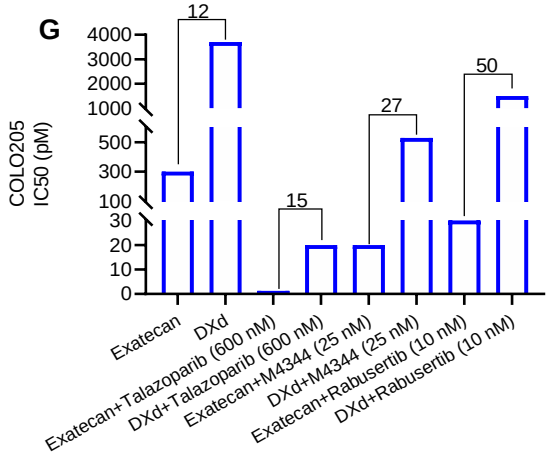

H

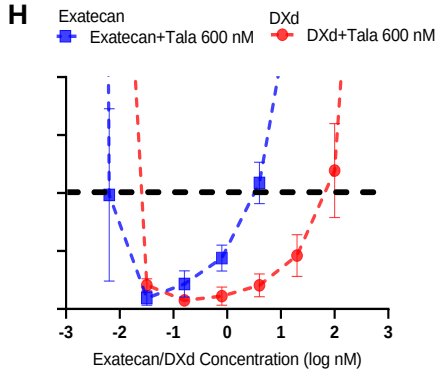

I

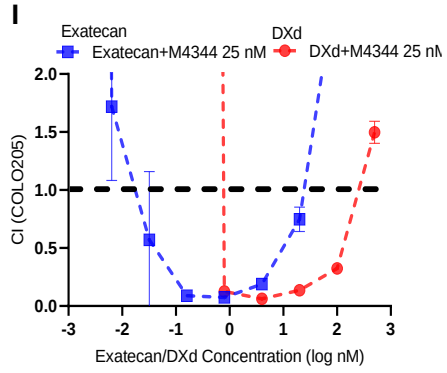

J

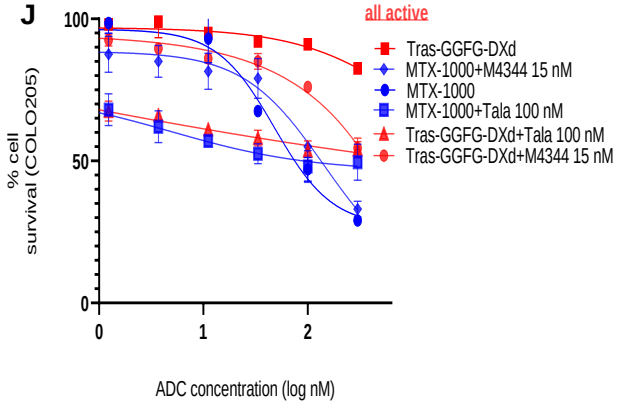

Supplementary Figure S18. A patient-derived xenograft (PDX) model with EGFR triple mutation.

A. Scheme of PDX establishment.
B. Summary of EGFR mutation in patient 200717 and PDX samples (P1 and P5).
C. Representative images of hematoxylin and eosin (H&E) of patient tumor (P0) and PDX passage 3 (P3). Images at 20X.
D. In vitro efficacy of EGFR/ALK TKI inhibitor alone and combination with cetuximab in in PDX 200717. Experimental details in Fig. 6.
E. Patient characteristics of PDX 200662. c-met amplification was detected by both IHC and FISH.
F. In vivo efficacy of EGFR inhibitor in 200662. Experimental details in Fig. 6.

A

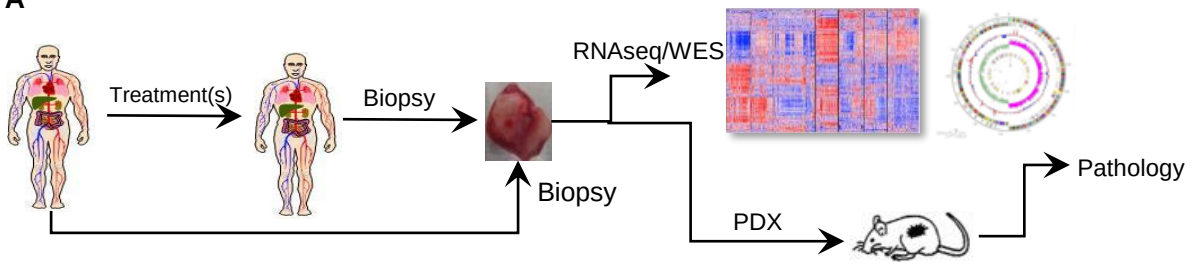

B

PDX 200717

- Derived from a 54-year old male patient: left upper lung primary bronchogenic carcinoma, adenocarcinoma; c-T2aN2M1b, stage IV
- Clinical NGS data: EGFR Ex19Δ 20%, T790M 9%, C797S 9%
- PDX model Pathology: Poorly - Moderately differentiated adenocarcinoma
- PDX model NGS data: : EGFR Ex19Δ 45.9%, T790M 17.37%, C797S 16.73%

Patient

EGFRR mutation	Allele freq (%)
Exon19 del	23.5
T790M	2.3

Post-AZD9291 treatment

EGFRR mutation	Allele freq (%)
Exon19 del	19.6
T790M	8.7
C797S	8.5

PDX

P1, NGS

EGFRR mutation	Allele freq (%)
Exon19 del	45.9
T790M	17.4
C797S	16.7

P5, Sanger sequencing

EGFR exon	mutation	AA change
18	-	-
19	GAATTAAGAGAAGCA deletion	746_750del
20	ACG-ATG, TGC-TCC	T790M, C797S
21	-	-

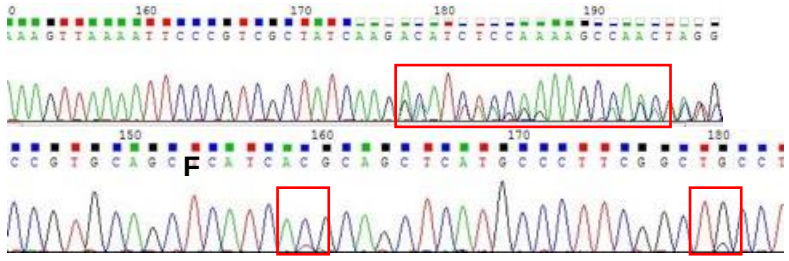

C

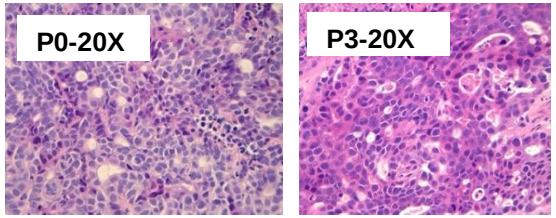

Pathology: Moderately differentiated adenocarcinoma (**Consistent with clinical diagnosis**)

D

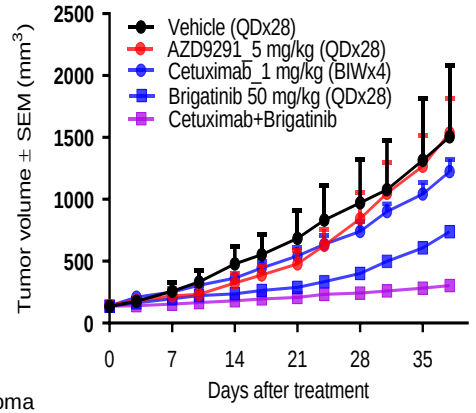

E

PDX 200662

- Derived from a 57-year old male patient: poorly differentiated adenocarcinoma of the right lower lung
- PDX model Pathology: Poorly - Moderately differentiated adenocarcinoma
- NGS and FISH data: EGFR 19del,c-met amplification
- Treatment history: Erlotinib and Osimertinib resistant

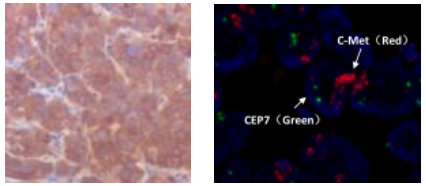

C-met amplification by IHC and FISH

F

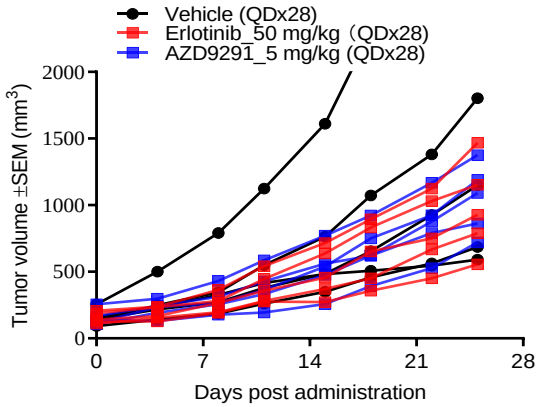

Supplementary Figure S19. MTX-1000 induces immunological cell death and enhances antitumor immunity of anti-PD-1.

A,B. Exatecan and MTX-1000 induce immunological cell death in vitro**.** HER2+ COLO205 cells were grown in 96-well and incubated with exatecan/DXd or ADC MTX-1000/Tras-GGFG-DXd for 48 hours at indicated concentration. Mitoxantrone was used as an ICD positive control. Calreticulin (CRT) translocation induced by exatecan and DXd (A) or MTX-1000 and Tras-GGFG-DXd to the cell surface was assessed by flow cytometry. Gating on PI staining allowed to exclude dead cells. A, Percentage of CRT positive cells. B. MFI of CRT. Data from 2 independent measurements. Unpaired two-sided t-test. **P*<0.05, ***P*<0.01, ****P*<0.001.

C. Cell viability after 48 hours of drug treatment. Cell number was counted by a cell counter.

D. Expression of exogenously introduced human HER2 gene was confirmed in mouse CT26 by flow cytometry. The HER2 expression on the CT26-hHER2 cells was medium (relative MFI of 30-50).

E. Combination effect of MTX-1000/Tras-GGFG-DXd and anti–PD-1 blocking antibody. In vivo effect of MTX-1000/Tras-GGFG-DXd (10 mg/kg, once a week, twice, i.v.) combined with anti–PD-1 antibody (5 mg/kg, twice a week, 2 cycles, i.v.) was compared with each agent individually in the immunocompetent mouse model inoculated with the CT26-hHER2 cells. Compounds were administered at the time points indicated by arrows.

F. Tumor growth inhibition from a combination treatment of MTX-1000/Tras-GGFG-DXd and anti–PD-1 blocking antibody. In vivo effect of MTX-1000/Tras-GGFG-DXd (10 mg/kg, once a week, twice, i.v.) combined with anti–PD-1 antibody (5 mg/kg, twice a week, 2 cycles, i.v.) was compared with each agent individually in the immunocompetent mouse (n=8) model inoculated with the CT26-hHER2 cells. Tras-GGFG-DXd–treated group was compared to MTX-1000, Tras-GGFG-DXd+PD-1. MTX-1000 was compared to Tras-GGFG-DXd and MTX-1000+PD-1 and PD-1 was compared to both Tras-GGFG-DXd+PD-1 and MTX-1000+PD-1. Tabulated result shown on the right. Unpaired two-sided t-test. **P*<0.05, ***P*<0.01, ****P*<0.001.

G. Body weight change of each animal group from Fig.7D.

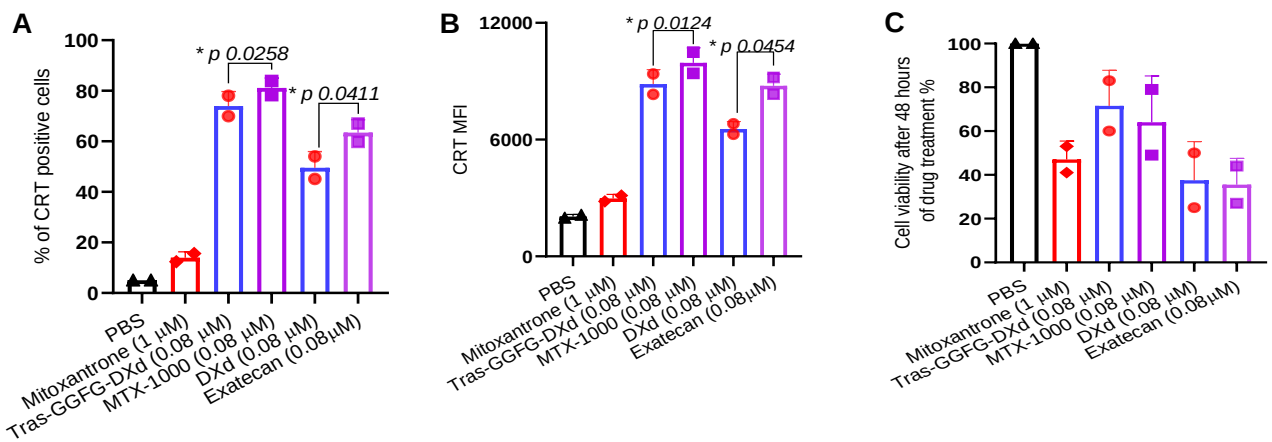

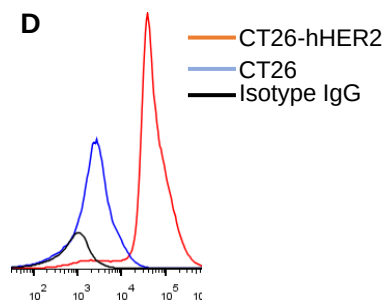

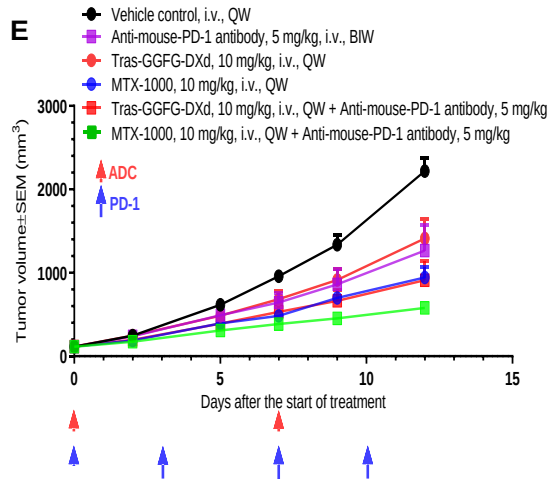

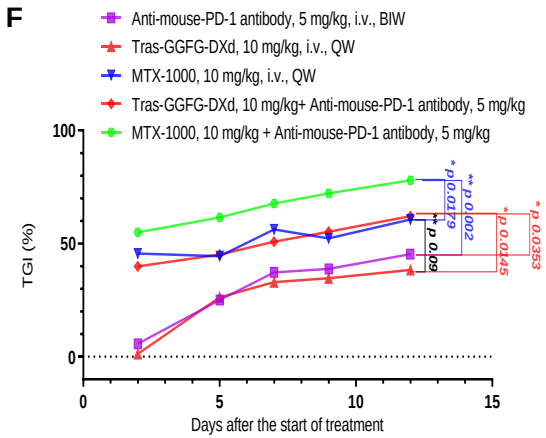

TGI	MTX-1000+PD-1
Tras-GGFG-DXd+PD-1	* p 0.0195

TGI	Tras-GGFG-DXd	PD-1	MTX-1000
MTX-1000	** p 0.09		
Tras-GGFG-DXd			** p 0.09
MTX-1000+PD-1		** p 0.002	* p 0.0179
Tras-GGFG-DXd+PD-1	* p 0.0145	* p 0.0353	n.s.